FLAME SHEET MODEL FOR A DIFFUSION-TYPE HF CHEMICAL LASER

Alexander A. Hayday

SCICOM, Incorporated

Prepared for:

Army Missile Research, Development and Engineering Laboratory

September 1973

UNCLASSIFIED
Security Classification

AD/A003316

DOCUMENT CONTROL DATA - R & D
(Security classification of title, body of abstract and indexing annotation must be entered when the overall report is classified)

1. ORIGINATING ACTIVITY (Corporate author)
SCICOM, Inc.
3313 Memorial Parkway SE
Huntsville, Alabama

2a. REPORT SECURITY CLASSIFICATION
Unclassified

2b. GROUP
N/A

3. REPORT TITLE
FLAME SHEET MODEL FOR A DIFFUSION-TYPE HF CHEMICAL LASER

4. DESCRIPTIVE NOTES (Type of report and inclusive dates)
Final Report

5. AUTHOR(S) (First name, middle initial, last name)
Alexander A. Hayday

6. REPORT DATE
September 1973

7a. TOTAL NO. OF PAGES
90

7b. NO. OF REFS
10

8a. CONTRACT OR GRANT NO.
DAAH01-72-C-1088

b. PROJECT NO.

c.

d.

9a. ORIGINATOR'S REPORT NUMBER(S)
RK-CR-73-1

9b. OTHER REPORT NO(S) (Any other numbers that may be assigned this report)
AD_____

10. DISTRIBUTION STATEMENT
Approved for public release; distribution unlimited.

11. SUPPLEMENTARY NOTES
None

12. SPONSORING MILITARY ACTIVITY
U. S. Army Missile Command
Redstone Arsenal, Alabama

13. ABSTRACT

This report presents a theory describing the flow field near the entrance to the cavity of a continuous wave chemical laser. The HF chemistry is considered in some detail but the point of view is general and applicable to other chemistries. The theory yields criteria for limiting flow regimes and establishes the influence of several key parameters explicitly. In particular, the important role played by the diluents in inhibiting collisional deactivation is discussed on the basis of the macroscopic flow equations. The theory rests on well-set Damkohler number arguments and established boundary layer concepts. The former lead to a classification of the relative importance of diffusion, momentum exchange mixing and finite rate kinetics when all three processes are simultaneously accounted for. Laminar and turbulent flows are treated on a unified basis; the latter are discussed from the phenomenological point of view. First approximations for the case of a diffusion flame are obtained and an appropriate perturbation technique describing collisional deactivation is developed. The diffusion limited case is shown to be a valid approximation to several systems now operating. Radiative interactions are considered for a medium near saturation. Possible rotational nonequilibrium effects are discussed briefly.

DD FORM 1 NOV 68 1473 REPLACES DD FORM 1473, 1 JAN 64, WHICH IS OBSOLETE FOR ARMY USE.

UNCLASSIFIED
Security Classification

14. KEY WORDS	LINK A		LINK B		LINK C	
	ROLE	WT	ROLE	WT	ROLE	WT
Chemical laser						
Diffusion						
Diffusion limited						
Mixing						
Boundary layer						

SUMMARY

This report presents a theory describing the flow field near the entrance to the cavity of a continuous wave chemical laser. The HF chemistry is considered in some detail but the point of view is general and applicable to other chemistries. The theory yields criteria for limiting flow regimes and establishes the influence of several key parameters explicitly. In particular, the important role played by the diluents in inhibiting collisional deactivation is discussed on the basis of the macroscopic flow equations. The theory rests on well-set Damkohler number arguments and established boundary layer concepts. The former lead to a classification of the relative importance of diffusion, momentum exchange mixing and finite rate kinetics when all three processes are simultaneously accounted for. Laminar and turbulent flows are treated on a unified basis; the latter are discussed from the phenomenological point of view. First approximations for the case of a diffusion flame are obtained and an appropriate perturbation technique describing collisional deactivation is developed. The diffusion limited case is shown to be a valid approximation to several systems now operating. Radiative interactions are considered for a medium near saturation. Possible rotational nonequilibrium effects are discussed briefly.

PREFACE

This technical report summarizes work performed by SCICOM, Inc. for the Army Missile Command, Redstone Arsenal, Alabama, under Contract DAAH01-72-C-1088. Mr. William Martin serves as technical monitor for this contract.

CONTENTS

Section I

INTRODUCTION

In the past few years considerable effort was devoted to theoretical and experimental studies of continuous wave chemical lasers. Extensive bibliographies on the subject may be found in papers by Hofland and Mirels [1], [2], and Skifstad [3]. The impetus for these studies is largely due to the fact that chemical lasers show promise for more or less direct conversion of chemical energy into that of coherent radiation; a large fraction of the energy released in a combustion process typified by the reaction $H_2+F \rightleftharpoons HF+H$ is momentarily stored in the higher vibrational levels of the product molecules (HF) and part of this energy is extractable as radiation. Moreover, because chemical lasers unlike others bypass the intermediate thermalization of chemical energy, they are potentially of superior efficiencies.

Theoretical works on HF lasers are typified by [1], [2] and [3]. The first paper deals with devices functioning in the diffusion limited regime and the second is concerned with the operation of lasers employing premixed reagents. Both studies employ a number of simplifying assumptions pertaining to chemical kinetics and fluid mechanics. These assumptions make closed form solutions describing flow, kinetics, and radiative interaction in the cavity possible. Elaborate numerical solutions pertaining to the same problems are exemplified in the papers by King and Mirels [4], Thoenes, Ratliff and Benefield [5] and references quoted therein.

This technical report is conceptually related to [2] and [3] in that it deals with the development of analytical models describing the flow and radiation phenomena in the cavity of a continuous wave HF-chemical laser. Emphasis is

placed on interactions of initially separated streams of fuel and oxydizer and the resultant flame in the diffusion limited regime. Nonetheless, some of the results have more general validity.

The basic flow configuration is sketched in Fig.1., Page 85. Two initially separate, semi-infinite parallel streams of different velocities but equal pressures are brought into contact at x=0. One stream contains atomic fluorine and a diluent; the other consists of molecular hydrogen and a diluent or pure hydrogen. Either laminar or turbulent mixing and chemical interactions of the two streams commence aft of x=0.

The analysis is divided into several parts. In Section 2.1 radiative interactions are neglected and the flow and kinetics phenomena taking place in the mixing layer are examined within the framework of boundary layer theory. Laminar and turbulent mixing are treated on a unified basis from the phenomenological point of view. The mixture is taken to consist of the species HF(0), HF(1), HF(2), HF(3), H_2,F,H and two diluents, He or N_2. Apart from the pumping reactions creating HF(v) in the first three vibrational levels, only the dominant vibration - translation (V-T) deactivation reactions are included. The validity of the difusion flame model is established by considering the magnitudes of a set of Damkohler numbers characterizing the pumping reactions. Section 2.2 summarizes the zero order solutions, i.e, flame sheet solutions with collisional deactivation neglected. Some implications of these solutions are discussed in Section 2.3. Collisional deactivation phenomena are governed by a set of perturbation equations derived in Section 2.4. The latter equations are

given to second order in terms of a set of Damkohler numbers characterizing the V-T processes. The boundary value problems are set up for straight-forward numerical solutions. In Section 2.5, radiative interactions are considered for a medium near saturation. The question of rotational equilibrium is also briefly discussed.

Section 2

ANALYSIS

2.1 Flow Model and Kinetics

The starting point is the set of differential equations expressing respectively global conservation of mass, linear momentum, mass of individual species and total energy. With terms describing the influence of the radiation field excluded, the boundary layer form of this set is the following:

$$(\rho u)_x + (\rho v)_y = 0 \tag{1}$$

$$\rho u u_x + \rho v u_y = (\mu u_y)_y \tag{2}$$

$$\rho u (Y_i)_x + \rho v (Y_i)_y = \left[\rho D (Y_i)_y\right]_y \tag{3}$$

$$\rho u (h_{tf})_x + \rho v (h_{tf})_y = \left\{ \frac{\mu}{Pr}\left[(h_{tf})_y + \sum_{i=1}^{N} (Le_i - 1) h_{if} (Y_i)_y - (Pr - 1)\left(\tfrac{1}{2} u^2\right)_y\right]\right\}_y - \sum_{i=1}^{N} \dot{w}_i h_i^{\circ} \tag{4}$$

Equations (1)-(4) apply formally to turbulent flows provided ρ, u, v, Y_i, h_{tf} are interpreted as average quantities and the transport coefficients are identified with the "eddy" counterparts of those in laminar flows. The subscripts x and y denote partial derivatives. Otherwise, the notation is standard and summarized in the Nomenclature.

Reactions chosen to represent the kinetics are those used in [6] and values of the reaction rate constants, $k=aT^{b}\exp(-c/T)$ in $cm^3/gm\text{-}mole\text{-}sec$ are taken from [1].

Reaction		-ΔH(kcal/g-mole)	a	b	c°K
0.	$H_2 + F \underset{k_{b,0}}{\overset{k_{f,0}}{\rightleftharpoons}} HF(0) + H$	+ 31.52	$0.7\cdot10^{13}$	0	860
1.	$H_2 + F \rightarrow HF(1) + H$	+ 20.23	$1.4\cdot10^{13}$	0	860
2.	$H_2 + F \rightarrow HF(2) + H$	+ 9.40	$7.0\cdot10^{13}$	0	860
3.	$H_2 + F \rightarrow HF(3) + H$	+(-0.94)	$0.7\cdot10^{13}$	0	860
4.	$HF(3) + M_c \rightarrow HF(2) + M_c$	+ 10.34	$1.5\cdot10^{6}$	1.3	0
5.	$HF(2) + M_c \rightarrow HF(1) + M$	+ 10.83	$1.0\cdot10^{6}$	1.3	0
6.	$HF(1) + M_c \rightarrow HF(0) + M_c$	+ 11.18	$0.5\cdot10^{6}$	1.3	0

The first four reactions define chemical pumping. For the conditions pertinent to lasers, they are predominantly forward and therefore the backward rates are neglected. Reactions 4-6 are taken as dominant for the vibration-translation (V-T) collisional deactivation processes. Vibration-vibration (V-V) transfers, say those competing in deactivating the 1/0 band, may be included without substantial complications. The latter are not considered herein because they are primarily responsible for redistribution of energy among the different v-levels (thermalization). Heats of reactions are given in kcal/g-mole and, for reactions 0-3, imply an average difference of 10.86 kcal/g-mole per vibrational level.

The mixture consists of species HF(0), HF(1), HF(2), HF(3), H_2, F, H and at most two diluents D_1 and D_2. The species are numbered from 0 to 8. However, for emphasis, occasional use of chemical symbols as subscripts is made. For example $Y_4 \equiv Y_{H_2}$, $M_5 \equiv M_F$, $Y_{HF,2} \equiv Y_2$ and so on. While the kinetic model is representative and chosen more or less for convenience, it nevertheless covers the main phenomena of interest.

Based upon the law of mass action, the nine species–seven reactions system of diffusion equations (3) is the following:

$$\rho u (Y_0)_x + \rho v (Y_0)_y = \left[\rho D (Y_0)_y\right]_y + k_{f,0} \frac{Y_4}{M_{H_2}} \frac{Y_5}{M_F} M_{HF} + k_{f,6} \rho^2 \frac{Y_1}{M_{HF}} \frac{Y_6}{M_6} M_{HF} - 0 \; ; \quad (6)$$

$$\rho u (Y_1)_x + \rho v (Y_1)_y = \left[\rho D (Y_1)_y\right]_y + k_{f,1} \rho^2 \frac{Y_4}{M_{H_2}} \frac{Y_5}{M_F} M_{HF} + k_{f,5} \rho^2 \frac{Y_2}{M_{HF}} \frac{Y_6}{M_6} M_{HF} - k_{f,6} \rho^2 \frac{Y_1}{M_{HF}} \frac{Y_6}{M_6} M_{HF} \; ; \quad (7)$$

$$\rho u (Y_2)_x + \rho v (Y_2)_y = \left[\rho D (Y_2)_y\right]_y + k_{f,2} \rho^2 \frac{Y_4}{M_{H_2}} \frac{Y_5}{M_F} M_{HF} + k_{f,4} \rho^2 \frac{Y_3}{M_{HF}} \frac{Y_6}{M_6} M_{HF} - k_{f,5} \rho^2 \frac{Y_2}{M_{HF}} \frac{Y_6}{M_6} M_{HF} \; ; \quad (8)$$

$$\rho u (Y_3)_x + \rho v (Y_3)_y = \left[\rho D (Y_3)_y\right]_y + k_{f,3} \rho^2 \frac{Y_4}{M_{H_2}} \frac{Y_5}{M_F} M_{HF} + 0 - k_{f,4} \rho^2 \frac{Y_3}{M_{HF}} \frac{Y_6}{M_6} M_{HF} \; ; \quad (9)$$

$$\rho u (Y_4)_x + \rho v (Y_4)_y = \left[\rho D (Y_4)_y\right]_y - \rho^2 \left(\sum_{i=0}^{3} k_{f,i} \right) \frac{Y_4}{M_{H_2}} \frac{Y_5}{M_F} M_{H_2} \; ; \quad (10)$$

$$\rho u (Y_5)_x + \rho v (Y_5)_y = \left[\rho D (Y_5)_y\right]_y - \rho^2 \left(\sum_{i=0}^{3} k_{f,i} \right) \frac{Y_4}{M_{H_2}} \frac{Y_5}{M_F} M_F \; ; \quad (11)$$

$$\rho u (Y_6)_x + \rho v (Y_6)_y = \left[\rho D (Y_6)_y\right]_y + \rho^2 \left(\sum_{i=0}^{3} k_{f,i} \right) \frac{Y_4}{M_{H_2}} \frac{Y_5}{M_F} M_H \; ; \quad (12)$$

$$\rho u (Y_7)_x + \rho v (Y_7)_y = \left[\rho D (Y_7)_y\right]_y \; ; \quad (13)$$

$$\rho u (Y_8)_x + \rho v (Y_8)_y = \left[\rho D (Y_8)_y\right]_y . \quad (14)$$

The mass fraction Y_c is connected with the collision partner of molecular weight M_c in the reactions 4-6. Herein, the latter is HF or H or a suitable average of the two.

Define

$$Y_{HF,tot} \equiv \sum_{i=0}^{3} Y_i \tag{15}$$

and sum equations (6)-(9). Then, irrespective of the magnitude of the terms accounting for collisional deactivation, the result is

$$\rho u \left(Y_{HF,tot}\right)_x + \rho v \left(Y_{HF,tot}\right)_y = \left[\rho D \left(Y_{HF,tot}\right)_y\right]_y + \rho^2 \left(\sum_{i=0}^{3} k_{f,i}\right) \frac{Y_{H_2}}{M_{H_2}} \frac{Y_F}{M_F} M_{HF}. \tag{16}$$

If now $Y^o_{HF,v}$ denotes the HF mass fraction in the level v when collisional deactivation is neglected, then any one of the equations (6)-(9) is of the form

$$\rho u \left(Y^o_{HF,v}\right)_x + \rho v \left(Y^o_{HF,v}\right)_y = \left[\rho D \left(Y^o_{HF,v}\right)_y\right]_y + \rho^2 k_{f,v} \frac{Y_{H_2}}{M_{H_2}} \frac{Y_F}{M_F} M_{HF}. \tag{17}$$

An immediate consequence of (16) and (17) is that

$$Y^o_i = Y^o_{HF,v} = f_v Y_{HF,tot} \qquad v = i, \; v = 0,1,2,3, \tag{18}$$

where the ratios $f_v \equiv k_{f,v} / \sum_{v=0}^{3} k_{f,v}$ are constants. But, insofar as this section is concerned, each $Y^o_{HF,v}$ is altered solely by the neglected terms. Therefore, it is natural to examine conditions for the validity of expansions

$$Y_{HF,v} = Y^o_{HF,v} + \zeta_{cd,v} Y^{(1)}_{HF,v} + \zeta^2_{cd,v} Y^{(2)}_{HF,v} + \text{interaction terms} \tag{19}$$

where each $\zeta_{cd,v}$ is a parameter characterizing collisional deactivation of a given v-level and where the interaction terms specify the same type of influence exerted by the higher vibrational levels. The latter will be referred to as secondary pumping terms because they will represent the supply of an excited specie into level v resulting from collisional deactivation of level v+1. The explicit structure of the expansion (19) is to be determined. For the moment, (19) is regarded as a formalism wherein each $\zeta_{cd,v}$ is a member of a set of collisional deactivation Damkohler numbers. Each such number is a ratio of two characteristic times, τ_{flow}/τ_{chem}. This set and its pumping counterpart, taken together, determine the structure of the chemically active mixing zone. Now, in a diffusion controlled laser device, the primary pumping Damkohler numbers, namely those associated with reactions 0-3, exceed the $\zeta_{cd,v}$'s by orders of magnitude. (In any case, the magnitude of the former ought to be large for efficient H_2-F combustion.) Therefore, it is logical to inquire about conditions whereat the magnitude of the primary pumping Damkohler numbers is great enough to assure combustion in a narrow flame zone. In such cases $Y^o_{HF,v}$ is a simple linear function of u alone, provided the momentum equation (2) is decoupled from the rest of the system.

The matters just brought up are best clarified by the governing equations themselves subject to a transformation of the similarity class. It is convenient to indicate first the procedure for decoupling the momentum equation governing laminar flows. Changes required for handling turbulent flows are summarized in Footnote 1.

Let

$$x,y \to s,\hat{\eta};\quad s=(\rho_e\mu_e)u_e x,\quad \hat{\eta}=\frac{u_e}{(2s)^{1/2}}\int_0^y \rho\, dy \qquad (20)$$

denote a similarity-like mapping and let

$$\Psi = (2s)^{1/2}\hat{f}(s,\hat{\eta}) \tag{21}$$

stand for the stream function such that $\rho u=\Psi_y$ and $\rho v=-\Psi_x$. Then (20) together with (21) yield (2) in the form

$$\left[\left(\frac{\rho\mu}{\rho_e\mu_e}\right)\hat{f}_{\hat{\eta}\hat{\eta}}\right]_{\hat{\eta}} + \hat{f}\hat{f}_{\hat{\eta}\hat{\eta}} = 2s\left(\hat{f}_{\hat{\eta}s}\hat{f}_{\hat{\eta}} - \hat{f}_{\hat{\eta}\hat{\eta}}\hat{f}_s\right). \tag{22}$$

In terms of

$$f = l^{1/2}\hat{f}, \quad \eta = l^{-1/2}\hat{\eta}, \quad l \equiv \frac{\rho\mu}{\rho_e\mu_e} = \text{const} \tag{23}$$

the foregoing equation is equivalent to

$$f_{\eta\eta\eta} + ff_{\eta\eta} = 2s\left(f_{\eta s}f_{\eta} - f_s f_{\eta\eta}\right). \tag{24}$$

The boundary conditions imposed on (2) are

$$\lim_{y\to\infty} u(x,y) = u_e, \quad \lim_{y\to-\infty} u(x,y) = u_e.$$

and imply that $f=f(\eta)$ alone. The boundary value problem is

$$\begin{gathered} f''' + ff'' = 0 \\ \lim_{\eta\to\infty} f'(\eta) = 1, \quad \lim_{\eta\to-\infty} f'(\eta) = \Lambda \equiv \frac{u_e}{u_e}, \quad f(0) = 0 \end{gathered} \tag{25}$$

where $' \equiv \frac{d}{d\eta}$.[1)]

Consider now the system of diffusion equations under the s,η transformation. Expressed in dimensionless form, this system generates the requisite Damkohler numbers once a suitable set of reference conditions is chosen. The choice is of some importance: one reason is that it affects the estimates of pumping and collisional deactivation lengths. This is illustrated in the next few paragraphs.

In the s,η variables, the diffusion equations governing transports of fuel H_2 and oxydizer F take the form

---

[1)] The turbulent flow analogue is obtained as follows. Let

$$\mu \equiv \mu_t = \rho\varepsilon \ , \quad \mu_{t,e} = \rho_e \varepsilon_o \ , \quad \varepsilon_o = \text{const} ; \tag{i}$$

$\varepsilon = \varepsilon(x) = \varepsilon_o e(x)$ is an eddy diffusivity. Set

$$\bar{s} = \rho_e^2 \varepsilon_o u_e \xi \ , \quad \hat{\eta} = \frac{u_e}{(2\bar{s})^{1/2}} \int_o^y \rho \, dy \ . \tag{ii}$$

where $\xi = \int_o^x e(x)dx$. As before, $\Psi = (2\bar{s})^{-1/2} \hat{f}(\bar{s},\hat{\eta})$. Under (ii), the the analogue of (22) is

$$\left[\left(\frac{\rho}{\rho_e}\right)^2 \hat{f}_{\hat{\eta}\hat{\eta}}\right]_{\hat{\eta}} + \hat{f}\hat{f}_{\hat{\eta}\hat{\eta}} = 2\bar{s}\left(\hat{f}_{\hat{\eta}\bar{s}}\hat{f}_{\hat{\eta}} - \hat{f}_{\hat{\eta}\hat{\eta}}\hat{f}_{\bar{s}}\right). \tag{iii}$$

This equation may be handled in several ways. One procedure is to replace the ratio ρ/ρ_e by a suitable constant average and then to introduce the obvious analogue of (23). This approach reproduces the Blasius problem (25). Other possibilities are open. The same procedure may be applied to the other equations. Therefore it suffices to discuss the laminar case alone.

$$(\bar{Y}_4)_{\eta\eta} + Sc\, f(\bar{Y}_4)_\eta - Sc\left[\frac{2x}{u_e}\left(\rho\sum_{i=0}^{3} k_{f,i}\right)\frac{Y_{5,e}}{m_F}\right]\bar{Y}_4\bar{Y}_5$$

$$= 2Sc\,(\rho_e\mu_e)u_e x\left[f_\eta(\bar{Y}_4)_3 - f_3(\bar{Y}_4)_\eta\right] \qquad (26)$$

and

$$(\bar{Y}_5)_{\eta\eta} + Sc\, f(\bar{Y}_5)_\eta - Sc\left[\frac{2x}{u_e}\left(\rho\sum_{i=0}^{3} k_{f,i}\right)\frac{Y_{4,e^-}}{m_{H_2}}\right]\bar{Y}_4\bar{Y}_5 \qquad (27)$$

$$= 2Sc\,(\rho_e\mu_e)u_e x\left[f_\eta(\bar{Y}_5)_3 - f_3(\bar{Y}_5)_\eta\right].$$

The normalized mass fractions $\bar{Y}_4$ and $\bar{Y}_5$ are defined as

$$\bar{Y}_4 \equiv \frac{Y_4 - Y_{4,*}^{\circ}}{Y_{4,e^-} - Y_{4,*}^{\circ}} = \frac{Y_4}{Y_{4,e^-}} \quad \text{and} \quad \bar{Y}_5 \equiv \frac{Y_5 - Y_{5,*}^{\circ}}{Y_{5,e} - Y_{5,*}^{\circ}} = \frac{Y_5}{Y_{5,e}}. \qquad (28)$$

The equality follows because $Y_{4,*}^{\circ}$ and $Y_{5,*}^{\circ}$ being identified with the zero order solutions (subscript o) at the combustion interface (subscript $*$) are both zero.[2)]

---

2) The reference states denoted by an asterisk ($*$) are based upon solutions to the flame sheet problem discussed in 2.2 of this section. This slight circularity in logic is unimportant because, in all cases, a posteriori verification of the validity of the flame sheet model is made. It is possible to think of the $*$-reference states as associated with an assumed flame sheet. The appropriateness of this model is then verified (or negated) a posteriori. The $*$-reference states are used for all species whose mass fractions vanish at the outer edges of the mixing zones.

The differential equations (26) and (27) generate two primary pumping Damkohler numbers $\zeta_{p,4}$ and $\zeta_{p,5}$:

$$Sc\left(\frac{2x}{u_e}\sum k_{f,i}\frac{Y_{s,e}}{M_r}\right)\bar{Y}_4\bar{Y}_5 = Sc\left(\frac{2x}{u_e}\rho_{ref,4}\sum a_i\frac{Y_{s,e}}{M_r}\right)\frac{\rho}{\rho_{ref,4}}e^{-\frac{c}{T}}\bar{Y}_4\bar{Y}_5$$

$$= Sc\left(\frac{2x}{u_e}\rho_{ref,4}\sum a_i'\frac{Y_{s,e}}{M_r}\right)\frac{\rho}{\rho_{ref,4}}e^{-\frac{c}{T_{ref}}\left(1-\frac{1}{\theta}\right)}\bar{Y}_4\bar{Y}_5 = Sc\,\zeta_{p,4}\frac{\rho}{\rho_{ref,4}}e^{-\frac{c}{T_{ref}}\left(1-\frac{1}{\theta}\right)}\bar{Y}_4\bar{Y}_5, \quad (29)$$

$$Sc\left(\frac{2x}{u_e}\rho\sum k_{f,i}\frac{Y_{4,e^-}}{M_{N_2}}\right)\bar{Y}_4\bar{Y}_5 = Sc\left(\frac{2x}{u_e}\rho_{ref,5}\sum a_i\frac{Y_{4,e^-}}{M_{N_2}}\right)\frac{\rho}{\rho_{ref,5}}e^{-\frac{c}{T}}\bar{Y}_4\bar{Y}_5$$

$$= Sc\left(\frac{2x}{u_e}\rho_{ref,5}\sum a_i'\frac{Y_{4,e^-}}{M_{N_2}}\right)\frac{\rho}{\rho_{ref,5}}e^{-\frac{c}{T_{ref}}\left(1-\frac{1}{\theta}\right)}\bar{Y}_4\bar{Y}_5 = Sc\,\zeta_{p,5}\frac{\rho}{\rho_{ref,5}}e^{-\frac{c}{T_{ref}}\left(1-\frac{1}{\theta}\right)}\bar{Y}_4\bar{Y}_5. \quad (30)$$

In (29) and (30) $a_i' \equiv a_i e^{-c/T_{ref}}$ and $\theta \equiv T/T_{ref}$. The procedure used here departs slightly from that given, for example, in [7,Chap.V] in that the Damkohler numbers are based upon the a_i''s and not the a_i's. This insures the functionally correct temperature dependence in the ζ_p's. It is noted that the left hand sides of (29) and (30) are related to the chemical source terms $\dot{w}_i/\rho$ written in the form $\dot{w}_i/\rho = (1/\tau_{chem})\omega_i(T,Y_i,P)$ where the ω_i's are dimensionless. The similarity mapping automatically introduces $\tau_{flow} \sim x/u_e$ and the ratios τ_{flow}/τ_{chem} are then identified as Damkohler numbers. The notation is meant to imply that $\zeta_{p,i}$ is a pumping ζ (subscript p) generated by the i^{th} specie diffusion equation (subscript i).

Estimates of characteristic lengths associated with primary chemical pumping, $x_{p,i}$, are obtained from $\zeta_{p,i}=1$, once a reference

state is chosen. Let the reference states for (26) and (27) be those used in (28), i.e. those corresponding to the respective free-stream conditions. Then $\zeta_{p,4}=1$ and $\zeta_{p,5}=1$ give

$$x_{p,4} = \frac{1}{Sc}\,\frac{\nu_e}{2}\,\frac{1}{\sum_{i=0}^{2} a_i'}\,\frac{M_F}{\rho_e - Y_{F,e}} \tag{31}$$

and

$$x_{p,5} = \frac{1}{Sc}\,\frac{u_e}{2}\,\frac{1}{\sum_{i=0}^{2} a_i'}\,\frac{M_{H_2}}{\rho_e Y_{4,e-}} \,. \tag{32}$$

For the representative conditions

$$u_e = 2\cdot 10^5 \text{ cm}, \quad Y_{F,e} = 0.1, \quad Y_{4,e-} = 1, \quad Y_{7,e} = Y_{H_2,e} = 0.9$$

$$p_e = p_{e-} = 1\cdot 10^{-2} \text{ atm}, \quad T_e = T_{e-} = 400^\circ\text{K} \text{ and } Sc = 1$$

the results are $x_{p,4}=2.7$ cm and $x_{p,5}=2.1\cdot 10^{-3}$ cm. A slight degree of arbitrariness exists depending upon the choice of the reference flow speed and depending upon whether the mixture Schmidt number Sc is incorporated in the Damkohler numbers or not. It is possible, for example, to use u_{e-} as the reference speed for the H_2-diffusion equation or an average reference speed $u_{ave} \equiv (u_e + u_{e-})/2$ can be introduced for all of the diffusion equations. From a practical standpoint, these matters are trivial because in laser applications u_e and u_{e-} rarely differ by more than a factor of three and the Schmidt numbers are not drastically different from unity.

The intent here is to emphasize the thousandfold difference in pumping length estimates. The large difference occurs because $(M_F/\rho_{e^-}Y_{5,e})\simeq 10^3(M_{H_2}/\rho_e Y_{4,e^-})$. The implications are that: a) the choice of the reference state is important in estimating chemical pumping lengths and that b) the Damkohler numbers based upon free-stream conditions are not necessarily indicative of local values in the combustion zone.[3)]

Evidently, more reliable estimates of $x_{p,i}$ and the companion collisional deactivation lengths $x_{cd,i}$ require a choice of a reference state reflecting the actual combustion zone conditions as closely as possible. This dictates the use of the diffusion equation for the excited species. An additional reason is that a relative comparison of chemical pumping lengths and collisional deactivation lengths is sought. The collisional deactivation Damkohler numbers appear in these equations but not in (26) and (27).

Under the s,η transformation, the diffusion equation for $Y_{HF_3} \equiv Y_3$ takes the form

$$(Y_3)_{\eta\eta} + Sc f (Y_3)_\eta + Sc \frac{2x}{u_e}\rho k_{f,3}\frac{Y_4}{m_{H_2}}\frac{Y_5}{m_F} m_{HF} - Sc \frac{2x}{u_e}\rho k_{f,4}\frac{Y_3}{m_{HF}}\frac{Y_5}{m_c} m_{HF} \tag{33}$$

$$= 2Sc\cdot s\left[f_\eta (Y_3)_s - f_s (Y_3)_\eta\right].$$

The logical normalization quantity is $Y^\circ_{3,*}$ – the zero order mass fraction of the HF specie generated at the combustion interface in the third vibrational level. The normalized form

---

3) In fact, Chung et al. [8] have shown that b) is directly related to possible combustion anomalies manifested by multiplicities of solutions in transitions from frozen to equilibrium flows. The anomalies are the more likely to occur the more exothermic the reaction.

of (33) is then

$$(\bar{Y}_3)_{\eta\eta} + Sc f(\bar{Y}_3)_\eta + Sc\left(\frac{2x}{u_e}\rho_*^\circ a_3' \frac{Y_{3,e}}{M_{H_2}} \frac{Y_{F,e}}{M_F} \frac{M_{HF}}{Y_{3,*}^\circ}\right)\frac{\rho}{\rho_*^\circ} e^{-\frac{\varepsilon}{T_*^\circ}\left(\frac{1}{\theta}-1\right)} \bar{Y}_4 \bar{Y}_5$$

$$- Sc\left[\frac{2x}{u_e}\rho_*^\circ (T_*^\circ)^b a_4 \frac{1}{M_{HF}} \frac{Y_{c,*}^\circ}{M_c} M_{HF}\right]\left(\frac{T}{T_*^\circ}\right)^b \frac{\rho}{\rho_*^\circ} \bar{Y}_3 \bar{Y}_c = 2Sc\cdot s\left[f_\eta(Y_3)_s - f_s(Y_3)_\eta\right]. \tag{34}$$

In accord with choosing $Y_{3,*}^\circ$ as the normalizing quantity, the reference states for the density and temperature, ρ_*° and T_*°, correspond to the zero order solutions at the flame sheet as well.

The analogue of (33) for $Y_{HF,2} \equiv Y_2$ is

$$(Y_2)_{\eta\eta} + Sc f(Y_2)_\eta + Sc \frac{2x}{u_e}\rho k_{f,2} \frac{Y_1}{M_{H_2}} \frac{Y_3}{M_F} M_{HF} + Sc \frac{2x}{u_e}\rho k_{f,4} \frac{Y_3}{M_{HF}} \frac{Y_c}{M_c} M_{HF}$$

$$- Sc \frac{2x}{u_e}\rho k_{f,5} \frac{Y_2}{M_{HF}} \frac{Y_c}{M_c} M_{HF} = 2Sc\cdot s\left[f_\eta(Y_2)_s - f_s(Y_2)_\eta\right] \tag{35}$$

and the same procedure which led to (34) now gives

$$(\bar{Y}_2)_{\eta\eta} + Sc f(\bar{Y}_2)_\eta + Sc\left(\frac{2x}{u_e}\rho_*^\circ a_2' \frac{Y_{3,e}}{M_{H_2}} \frac{Y_{F,e}}{M_F} \frac{M_{HF}}{Y_{2,*}^\circ}\right)\frac{\rho}{\rho_*^\circ} e^{-\frac{\varepsilon}{T_*^\circ}\left(\frac{1}{\theta}-1\right)} \bar{Y}_4 \bar{Y}_5$$

$$+ Sc\left[\frac{2x}{u_e}\rho_*^\circ (T_*^\circ)^b a_4 \frac{Y_{3,*}^\circ}{M_{HF}} \frac{Y_{c,*}^\circ}{M_c} M_{HF} \frac{1}{Y_{3,*}^\circ}\right]\left(\frac{T}{T_*^\circ}\right)^b \frac{\rho}{\rho_*^\circ} \bar{Y}_3 \bar{Y}_c \tag{36}$$

$$- Sc\left[\frac{2x}{u_e}\rho_*^\circ (T_*^\circ)^b a_5 \frac{1}{M_{HF}} \frac{Y_{c,*}^\circ}{M_c} M_{HF}\right]\left(\frac{T}{T_*^\circ}\right)^b \frac{\rho}{\rho_*^\circ} \bar{Y}_2 \bar{Y}_c = 2Sc\cdot s\left[f_\eta(\bar{Y}_2)_s - f_s(\bar{Y}_2)_\eta\right].$$

The remaining equations are deduced in the same fashion and are therefore omitted.

The following observations are worthwhile because they set the stage for the perturbation procedure developed in Section 2.4. Upon summation, the unnormalized excited specie diffusion equations of the type (33) reproduce the s,η transform of (2). Clearly, this is not true of the normalized counterparts typified by (34).[4] The pertinent Damkohler numbers are the terms in the square brackets on the left hand sides of the normalized diffusion equations. Starting from the highest vibrational level, v=3, the following two sets are obtained:

$$
\begin{aligned}
&Sc\left[\frac{2x}{u_e}\rho_*^\circ a_3'\frac{\gamma_{4,e}^-}{M_{N_2}}\frac{\gamma_{5,e}}{M_F}\frac{M_{HF}}{\gamma_{3,*}^\circ}\right] \equiv Sc\,\xi_{p,3}\\
&Sc\left[\frac{2x}{u_e}\rho_*^\circ a_2'\frac{\gamma_{4,e}^-}{M_{N_2}}\frac{\gamma_{5,e}}{M_F}\frac{M_{HF}}{\gamma_{2,*}^\circ}\right] \equiv Sc\,\xi_{p,2}\\
&Sc\left[\frac{2x}{u_e}\rho_*^\circ a_1'\frac{\gamma_{4,e}^-}{M_{N_2}}\frac{\gamma_{5,e}}{M_F}\frac{M_{HF}}{\gamma_{1,*}^\circ}\right] \equiv Sc\,\xi_{p,1}\\
&Sc\left[\frac{2x}{u_e}\rho_*^\circ a_0'\frac{\gamma_{4,e}^-}{M_{N_2}}\frac{\gamma_{5,e}}{M_F}\frac{M_{HF}}{\gamma_{0,*}^\circ}\right] \equiv Sc\,\xi_{p,0}
\end{aligned}
\qquad (37)
$$

and

$$
\begin{aligned}
&Sc\left[\frac{2x}{u_e}\rho_*^\circ (T_*^\circ)^b a_4\frac{1}{M_{HF}}\frac{\gamma_{C,*}^\circ}{M_C}M_{HF}\right] = Sc\,\xi_{cd,3}\\
&Sc\left[\frac{2x}{u_e}\rho_*^\circ (T_*^\circ)^b a_5\frac{1}{M_{HF}}\frac{\gamma_{C,*}^\circ}{M_C}M_{HF}\right] = Sc\,\xi_{cd,2}\\
&Sc\left[\frac{2x}{u_e}\rho_*^\circ (T_*^\circ)^b a_6\frac{1}{M_{HF}}\frac{\gamma_{C,*}^\circ}{M_C}M_{HF}\right] = Sc\,\xi_{cd,1}.
\end{aligned}
\qquad (38)
$$

---

4) $\sum_{i=0}^{3}\gamma_i = \gamma_{HF,tot}$ $\qquad \sum_{i=0}^{3}\bar{\gamma}_i = \frac{\gamma_0}{\gamma_{0,*}^\circ} + \frac{\gamma_1}{\gamma_{1,*}^\circ} + \frac{\gamma_2}{\gamma_{2,*}^\circ} + \frac{\gamma_3}{\gamma_{3,*}^\circ} \neq \frac{\gamma_{HF,tot}}{(\gamma_{HF,tot})_*^\circ}$

The first set characterizes the action of the primary pumping reactions and the second set reflects collisional deactivation of levels v=3,2 and 1. Members of the second set play a dual role: in any normalized diffusion equation, a negative term containing a collisional deactivation Damkohler number is related to deactivation of the given level whereas an analogous term with a plus sign appearing in the same equation reflects the supply of the excited specie resulting from collisional deactivation of the next higher level. The latter term is associated with what is herein called secondary pumping. Now, each secondary pumping term is small in comparison to its primary counterpart and, in this sense, can be neglected. But each such term must be retained in the perturbation series because otherwise a contradiction arises in the mathematical model. It is noted in passing that the normalization of the s,η forms of the differential equations automatically introduces the correct temperature dependence into the ζ_{cd}'s and this in turn reinforces the choice of the a_i''s, i=0, 1, 2 and 3 for the ζ_p's.

Estimates of the various primary pumping and collisional deactivation lengths are based upon $Sc\zeta_{p,3}=Sc\zeta_{p,2}=Sc\zeta_{p,1}=\ldots=1$ and $Sc\zeta_{cd,3}=Sc\zeta_{cd,2}=Sc\zeta_{cd,1}=1$. For example, $Sc\zeta_{p,2}=1$ gives

$$Sc\,\chi_{p,2}=\frac{1}{Sc}\,\frac{u_e}{2}\,\frac{1}{a_2'}\,\frac{M_{N_2}}{Y_{4,e}}\,\frac{M_F}{Y_{5,e}}\,\frac{Y_{2,*}^{\circ}}{M_{HF}}\,\frac{1}{\rho_*^{\circ}} \tag{39}$$

Let now the representative conditions following (32) remain unaltered. Then, taking $T_*^{\circ}\simeq 600^{\circ}K$ and $Y_{2,*}^{\circ}=[k_2/\sum_{i=0}^{i=3}k_i]\,(Y_{HF,tot})_*=[a_2/\sum_{i=0}^{i=3}a_i](Y_{HF,tot})_*=0.0744$

gives $Sc \cdot x_{p,2} = 1.7 \cdot 10^{-3}$cm. [5] The companion estimates $x_{p,o}$, $x_{p,1}$ and $x_{p,3}$ differ very little from $x_{p,2}$. Moreover, when secondary pumping is neglected – which effect is indeed small for the reactions considered herein -- then the $x_{p,i}$'s are identical:

$$x_{p,o} = \frac{a_2'}{a_o'} \frac{Y_{o,*}^\circ}{Y_{2,*}^\circ} x_{p,2} = \frac{a_2'}{a_o'} \frac{k_o}{k_2} x_{p,2} = x_{p,2} = x_{p,4} = x_{p,3} = x_p \qquad (40)$$

Each of the foregoing $x_{p,i}$'s is quite close to $x_{p,4}$. Evidently, in this example, the free stream conditions in the F-stream are much closer to the actual flame front conditions than those prevailing in the H_2-stream.

The same procedure yields estimates for collisional deactivation lengths, $x_{cd,i}$. For example, $Sc\zeta_{cd,2} = 1$ gives

$$x_{cd,2} = \frac{1}{Sc} \frac{u_e}{2} \frac{1}{a_4} \frac{1}{(T_*^\circ)^b} \frac{M_c}{Y_{c,*}^\circ} \frac{1}{\rho_*^\circ} \qquad (41)$$

which reduces to

$$x_{cd,2} = 0.512 \cdot 10^{-1} \frac{M_c}{Y_{c,*}^\circ} \text{ cm.} \qquad (42)$$

It remains to choose $M_c/Y^\circ_{c,*}$. For illustrative purposes, consider the same conditions which led to the $x_{p,2}$ estimates. The fluorine stream is highly diluted, there is little atomic hydrogen in the combustion zone and, therefore, in the first estimate, the collisional deactivation partner M_c is identified with HF_{total}. Hence, $M_c = 20$, $Y_{HF,tot} = Y^\circ_{c,*} = 0.104$ and $x_{cd,2} = 9.8$ cm. This value is large mainly because of the

[5] Zero order solutions show that $(Y_{HF,tot})_* = 0.104$ and $Y_{6,*} \equiv Y_{H,*} = 0.005$.

high degree of F-stream dilution and also because both T_e and T_{e^-} are low. In fact, $x_{cd,2}$ can easily decrease by more than an order of magnitude. This is demonstrated in Section 2.3. At this point, it will suffice to note that (41) clearly exhibits the influence exerted by several parameters upon a typical x_{cd} when convection, diffusion and kinetics are all simultaneously accounted for. In particular, (41) shows explicitly the crucial role played by a diluent in stretching x_{cd}. [6] The remaining estimates of $x_{cd,1}$ and $x_{cd,3}$ are obtained in the same way. With $M_c/Y^\circ_{c,*}$ fixed, the following relationships hold:

$$x_{cd,1} = \frac{a_5}{a_6} x_{cd,2} = 2 x_{cd,2} \quad \text{and} \quad x_{cd,3} = \frac{a_5}{a_4} x_{cd,2} = \frac{2}{3} x_{cd,2}. \tag{43}$$

---

6) While this hardly suggests any physical explanation for the actual role played by the diluent, the gross effect in stretching the x_{cd}'s as dictated by the macroscopic flow equations is as stated and worth noting. It is interesting to observe that $x_{p,2}$ (and hence each x_p) is roughly equal to that given in [1]. However, the estimates of the x_{cd}'s differ substantially from those of [1] mainly because of the factor $M_c/Y^\circ_{c,*}$ in (42). (The ratios $x_{p,2}/x_{cd,2}$ given here are about the same as in [1], provided one sets $M_c/Y^\circ_{c,*}=1$.) Herein, the factor $M_c/Y^\circ_{c,*}$ is taken to reflect the influence of the collisional deactivator through the molecular weight M_c; the degree of dilution and the molecular nature of the diluent strongly affect $Y^\circ_{c,*}$. For highly diluted F-streams the factor $M_c/Y^\circ_{c,*}$ may exceed one hundred. A few pertinent numerical values are given in Section 2.3.

2.2 The Flame Sheet Problem – Zero Order Solutions

The s,η transformed set of conservation equations governing the behavior of the mixture consisting of nine species undergoing the seven reactions (5) is the following:

$$f''' + ff'' = 0 \tag{44}$$

$$\bar{Y}_4^{o''} + f\bar{Y}_4^{o'} = 0 \tag{45}$$

$$\bar{Y}_5^{o''} + f\bar{Y}_5^{o'} = 0 \tag{46}$$

$$\bar{Y}_6^{o''} + f\bar{Y}_6^{o'} = 0 \tag{47}$$

$$\bar{Y}_{HF,tot}^{o''} + f\bar{Y}_{HF,tot}^{o'} = 0 \tag{48}$$

$$\bar{Y}_7^{o''} + f\bar{Y}_7^{o'} = 0 \tag{49}$$

$$\bar{Y}_8^{o''} + f\bar{Y}_8^{o'} = 0 \tag{50}$$

$$\bar{H}^{o''} + f\bar{H}^{o'} = 0 \tag{51}$$

$$Y_i^o \equiv Y_{HF,\sigma}^o = f_\sigma Y_{HF,tot}^o \; ; \; f_\sigma = \frac{a_\sigma}{\sum_{\nu=0}^{3} a_\nu} \; , \; i=\sigma=0,1,2,3. \tag{52}$$

Equations (45)-(51) were obtained from the s,η transforms of the basic differential equations (2)-(4) subject to the limiting conditions min $\zeta_{p,i} \to \infty$ and max $\zeta_{cd,i} \to 0$. The general basis for this limiting procedure is well known [7]. The standard and usually adequate simplification $Sc_i = Pr = Le_i = 1$ was employed to simplify matters further. For the convenience of the reader the normalized quantities $\bar{Y}_i$ and the dimensionless enthalpy function $\bar{H}$ defined in the Nomenclature are repeated

$$\bar{Y}_i \equiv \frac{Y_i}{Y_{i,w}^o}, \quad i = 0,1,2,3; \quad \bar{Y}_4^o \equiv \frac{Y_4^o}{Y_{4,e^-}}, \quad \bar{Y}_5^o \equiv \frac{Y_5^o}{Y_{5,e}}, \quad \bar{Y}_6^o \equiv \frac{Y_6^o}{Y_{6,w}^o}$$

$$\bar{Y}_7 \equiv \frac{Y_7^o}{Y_{7,e}}, \quad \bar{Y}_8 \equiv \frac{Y_8}{Y_{8,e^-}}, \quad \bar{H}^o \equiv \frac{h_{tf}^o}{h_{tf,e}}, \quad h_{tf} = \tfrac{1}{2}u^2 + \int_0^T c_p\,dT \simeq \tfrac{1}{2}u^2 + \bar{c}_p T. \tag{53}$$

Solutions of the one-parameter f-boundary value problem – Equation (44) subject to $f'(\infty)=1$, $f'(-\infty)=\Lambda$ and $f(0)=0$ – are available and solutions of the remaining differential equations can be expressed in terms of f'. Each is of the form

$$K_i(\eta) = A_i f'(\eta) + B_i \tag{54}$$

where the constants are evaluated from two-point boundary conditions. Now, a glance at the definitions (53) suffices to show that every equation in the system (45)-(50) satisfies zero-one boundary conditions. All zero order solutions fall into the similarity class and may be expressed as follows:

$$\bar{Y}_4^\circ = \frac{f' - f'_*}{\Lambda - f'_*} \quad \text{or} \quad Y_4^\circ = Y_{4,e} \frac{f' - f'_*}{\Lambda - f'_*}, \quad \eta_* \geq \eta > -\infty \tag{55}$$

$$\bar{Y}_5^\circ = \frac{f' - f'_*}{1 - f'_*} \quad \text{or} \quad Y_5^\circ = Y_{5,e} \frac{f' - f'_*}{1 - f'_*}, \quad \eta_* \leq \eta < \infty \tag{56}$$

$$\left.\begin{aligned} \bar{Y}_6^\circ &= \frac{f' - 1}{f'_* - 1} \quad \text{or} \quad Y_6^\circ = Y_{6,*} \frac{f' - 1}{f'_* - 1}, \quad \eta_* \leq \eta < \infty \\ \bar{Y}_6^\circ &= \frac{f' - \Lambda}{f'_* - \Lambda} \quad \text{or} \quad Y_6^\circ = Y_{6,*} \frac{f' - \Lambda}{f'_* - \Lambda}, \quad \eta_* \geq \eta > -\infty \end{aligned}\right\} \tag{57}_{a,b}$$

$$\left.\begin{aligned} \bar{Y}_{HF,tot}^\circ &= \frac{f' - 1}{f'_* - 1} \quad \text{or} \quad Y_{HF,tot}^\circ = \left(Y_{HF,tot}\right)_*^\circ \frac{f' - 1}{f'_* - 1}, \quad \eta_* \leq \eta < \infty \\ \bar{Y}_{HF,tot}^\circ &= \frac{f' - \Lambda}{f'_* - \Lambda} \quad \text{or} \quad Y_{HF,tot}^\circ = \left(Y_{HF,tot}\right)_*^\circ \frac{f' - \Lambda}{f'_* - \Lambda}, \quad \eta_* \geq \eta > -\infty \end{aligned}\right\} \tag{58}_{a,b}$$

$$\bar{Y}_7^\circ = \frac{f' - \Lambda}{1 - \Lambda} \quad \text{or} \quad Y_7 = Y_{7,e} \frac{f' - \Lambda}{1 - \Lambda}, \quad \text{all} \quad \eta \tag{59}$$

$$\bar{Y}_8^\circ = \frac{f' - 1}{\Lambda - 1} \quad \text{or} \quad Y_8 = Y_{8,e} \frac{f' - 1}{\Lambda - 1}, \quad \text{all} \quad \eta \tag{60}$$

and

$$\left.\begin{aligned} \bar{H}^\circ &= \frac{1 - \bar{H}_*^\circ}{1 - f'_*} f' + \frac{\bar{H}_*^\circ - f'_*}{1 - f'_*}, \quad \eta_* \leq \eta < \infty \\ \bar{H}^\circ &= \frac{\bar{H}_*^\circ - \bar{H}_e}{f'_* - \Lambda} f' + \frac{f'_* \bar{H}_e - \Lambda \bar{H}_*^\circ}{f'_* - \Lambda}, \quad \eta_* \geq \eta > -\infty \end{aligned}\right\} \tag{61}_{a,b}$$

A few points deserve mention. First of all, the results (55)-(61) are formalisms because they contain the unknowns $Y^{o}_{6,*}$, $(Y_{HF,tot})^{\circ}_{*}$, $\tilde{H}^{o}_{*}$, f'_{*} and the location parameter η_{*}. The latter quantities are determined from balance conditions and stoichiometry imposed at the interface. Second, for any set of (constant) free-stream conditions prescribed for the isobaric mixing layer, the quantities $Y_{HF,tot}$, Y_4, Y_5, Y_6, Y_7 and Y_8 remain functions of η alone and therefore the superscript o can be dropped from these variables. The physical implication is that in connection with the overall reaction $H_2+F \rightarrow HF+H$, the flow field is similar and fixed once and for all. In contrast, the distribution of HF among the vibrational levels and the associated energy distribution fall into the similarity class to zero order but not in general. Herein, the diffusion equations (45)-(50) and the energy equation (51) are not coupled with the momentum equation. (Coupling effects are in part accounted for through the various transformations.) Therefore, collisional deactivation destroys similarity essentially only in the Y_i's, i = 0, 1, 2 and 3. Finally, it is noted that the derivatives of the diluent mass fractions are continuous at the flame front. This is in accord with the physics of the model which demands that neither a source nor a sink for the diluents exist at η_{*}.

The relationships determining the unknowns $Y_{6,*}$, $(Y_{HF,tot})_{*}$ $\tilde{H}_{*}$, f'_{*} and the associated flame front location η_{*} are the following:

$$-\frac{1}{\mathcal{M}_{H_2}} Y_4' \Big|_{\eta_*^-} = \frac{1}{\mathcal{M}_F} Y_5' \Big|_{\eta_*^+} \tag{62}$$

$$\frac{1}{\mathcal{M}_{HF}} \left(-Y'_{HF,tot}\big|_{+} + Y'_{HF,tot}\big|_{-} \right) = \frac{1}{\mathcal{M}_H} \left(-Y_H'\big|_{+} + Y_H'\big|_{-} \right) \tag{63}$$

$$Y^{\circ}_{4,*} = Y^{\circ}_{5,*} \tag{64}$$

$$(Y_{HF,tot})_* + Y_{6,*} + Y_{7,*} + Y_{8,*} + Y_{4,*} + Y_{5,*} = 1 \tag{65}$$

and

$$-\left.h^{\circ\prime}_{tf}\right|_+ + \left.h^{\circ\prime}_{tf}\right|_- = -\frac{1}{M_{H_2}}\left.Y'_4\right|_- - \sum_{\nu=0}^{3} f_\nu \Delta H_\sigma \tag{66}$$

The first two statements, (62) and (63), are in accord with the stoichiometry of the overall reaction $H_2+F \rightarrow HF_{tot}+H$. Molar fluxes of H_2 and F are therefore equal at the flame front and the condition holds for the products H and HF_{tot}.[7] Moreover, both H_2 and F are destroyed at the combustion sheet, (64). Equation (65) is a standard mass balance condition and (66) is a local energy balance which states that energy conducted away from the interface is in balance with the energy generated by chemical reactions. The set $Y_{6,*}$, $(Y_{HF,tot})_*$, $\bar{H}^{\circ}_*$, f'_* and η_* is determined by combining (62)-(66) with (55)-(61). The procedure is given in the following paragraphs.

In view of (55) and (56), the stoichiometric requirement (62) implies that

$$f'_* = \frac{M_{H_2} Y_{5,e} \Lambda + M_F Y_{4,e}}{Y_{4,e} M_F + Y_{5,e} M_{H_2}} \tag{67}$$

---

[7] Note that the diffusion coefficients in (62) and (63) are taken as equal to one another. This is consistent with the assumptions $Le_i \equiv \frac{\rho D_i c_p}{k} = 1$ and $Pr \equiv \frac{\mu c_p}{k} = 1$ where each $D_i \equiv D_{ij}$ is a multi-component diffusion coefficient expressed in terms of the binary coefficients D_{ij} of the various pairs. Since $Sc_i \equiv \frac{Le_i}{Pr} = 1$, the D_i's are equal.

The relationship (67) is used as follows. The right-hand side is known and η_* is identified with the unique η-value corresponding to the now known f'. For example, η_* may be read off from available tabulations of $f'(\eta)$. In this sense, (67) determines both the flame front flow velocity component $u_*=u_e f'_*$ and the locations of the flame front.

Substituting the derivatives of (57) and (58) into (63) reduces the latter statement to

$$(Y_{HF,tot})_* = \frac{M_{HF}}{M_H} Y_{H,*} \quad . \tag{68}$$

This condition implies equality of mole fractions of HF_{tot} and and H at η_*. Now, a second equation relating $(Y_{HF,tot})_*$ and $Y_{H,*}$ is obtained by substituting (54), (59) and (60) evaluated at η_* together with $Y_{7,e}=1-Y_{5,e}$ and $Y_{8,e-}=1-Y_{4,e-}$ into (65) and eliminating f'_* via (67). The result is

$$Y_{H,*}+(Y_{HF,tot})_* + (1-Y_{5,e})\frac{M_F Y_{4,e-}}{Y_{4,e-}M_F + Y_{5,e}M_{H_2}} + (1-Y_{4,e-})\frac{Y_{5,e}M_{H_2}}{Y_{4,e-}M_F + Y_{5,e}M_{H_2}} = 1. \tag{69}$$

It follows from (68) and (69) that

$$(Y_{HF,tot})_* = \frac{M_{HF}}{M_{HF}+M_H} \cdot \frac{Y_{4,e-}-Y_{5,e}(M_F+M_{H_2})}{Y_{4,e-}M_F + Y_{5,e}M_{H_2}} = \frac{M_{HF}Y_{4,e-}-Y_{5,e}}{Y_{4,e-}M_F + Y_{5,e}M_{H_2}} \tag{70}$$

and

$$Y_{H,*} = \frac{M_H}{M_{HF}+M_H} \frac{Y_{4,e-}-Y_{5,e}(M_F+M_{H_2})}{Y_{4,e-}M_F + Y_{5,e}M_{H_2}} = \frac{M_H Y_{4,e-}-Y_{5,e}}{Y_{4,e-}M_F + Y_{5,e}M_{H_2}} \tag{71}$$

Formulae (70) and (71) indicate that the source strength for HF and H as reflected by the mass fractions $(Y_{HF,tot})_*$ and $(Y_H)_*$ is solely a function of the supply and molecular weights of H_2 and F. The absence of any λ-dependence is noted. This fact and the sum (65) suggest that at the combustion interface all mass fractions are independent of the momentum exchange parameter Λ. This is indeed the case and may be shown as follows. For each specie, $Y_{i,*}^{\circ}$ is given by one of the formulae (55)-(60) wherein $f'=f'_*$. The latter quantity is eliminated via (67) and the result is independent of Λ. For example:

$$Y_{7,*} = Y_{7,e}\,\frac{f'_* - \Lambda}{1-\Lambda} = Y_{7,e}\,\frac{M_F\,Y_{4,e}}{Y_{4,e}M_F + Y_{5,e}M_{H_2}} \,. \qquad (72)$$

Thus, momentum exchange mixing affects the location of the flame sheet and the shift in mass fraction profiles but not the mass fraction values at η_*.

It is noted in passing that at the combustion interface the local mass balance expressed in the s,η variables,

$$-Y'_{H_2}\big|_- + Y'_F\big|_+ + Y'_7\big|_+ - Y'_6\big|_- = -Y'_{HF,tot}\big|_+ + Y'_{HF,tot}\big|_- - Y'_H\big|_+ + Y'_H\big|_- + Y'_7\big|_+ - Y'_6\big|_+ \qquad (73)$$

reduces to an identity.[8] Equation (73) is obtained from a general balance by assuming that all diffusion coefficients are equal and constant; convective terms cancel out whenever f and f' are continuous at η_*.

---

8) This may be shown by substituting the derivatives of the set (55)-(60) together with the function values (67), (70) and (71) into (73).

The assumption of equal diffusion coefficients is subject to question in connection with chemical systems containing species of widely different molecular weights. This is the case for the diffusion controlled HF laser employing an N_2-diluted F-stream interacting with a pure H_2-stream. A rough estimate of the influence exerted by unequal diffusion coefficients on the structure of the mixing zone is obtained as follows. Let D_I and D_{II} denote respectively average constant values on the F and H_2 sides of the flame front. Suppose that $D_I \neq D_{II}$ but that all Schmidt numbers are still sufficiently close to unity so that Sc=1 can be retained in the differential equations. (While the foregoing statement is not entirely consistent, nonetheless, the results ought to indicate the correct trends.) The balance conditions (62) and (63) are generalized to include D_I and D_{II}. The new form of (62) together with (55) and (56) yields

$$f_F' = \frac{M_{H_2} Y_{5,e} \Lambda D_I + Y_{4,e} M_F D_{II}}{Y_{4,e} M_F D_I + Y_{5,e} M_{H_2} D_I} . \qquad (74)$$

The relationships (68), (70) and (71) remain unaltered. Therefore, the influence of unequal diffusion coefficients is similar to that of Λ in that both affect the flame front location and thereby shift the mass fraction profiles but otherwise leave the structure of the flame zone unchanged.

It remains to determine the total frozen enthalpy ratio $\tilde{H}_*^\circ$ and then obtain the expression for the zero order value of the flame front temperature T_*°. The formula for

$$\bar{H}_*^\circ = \frac{\bar{H}_e^- \frac{M_{HF}}{M_F} Y_{5,e} + \frac{M_{HF}}{M_{H_2}} Y_{4,e}^- + \frac{(M_{HF})^2}{M_F M_{H_2}} Y_{5,e} Y_{4,e}^- \left(\frac{1}{h_{f,e} M_{HF}} \sum_{\nu=0}^{3} f_\nu \Delta H_\nu \right)}{\frac{M_{HF}}{M_{H_2}} Y_{4,e}^- + \frac{M_{HF}}{M_F} Y_{5,e}} \tag{75}$$

is a straightforward consequence of (66), (55) and (61). The associated flame temperature T_*° follows from the definition

$$\bar{H}_*^\circ = \frac{\frac{1}{2} u_*^2 + \bar{c}_{p,*} T_*^\circ}{\frac{1}{2} u_e^2 + \bar{c}_p T_e} \tag{76}$$

where $u_* = f_*' u_e$ and $\int_0^T c_p \, dT = \bar{c}_p T$.

For equal diffusion coefficients, an alternate version of (67) and (75) is noted:

$$f_*' = \frac{\Lambda m_{5,e} + m_{4,e}^-}{m_{4,e}^- + m_{5,e}} \tag{77}$$

and

$$\bar{H}_*^\circ = \frac{\bar{H}_e^- m_{5,e} + m_{4,e}^- + m_{5,e} m_{4,e}^- \left(\frac{1}{h_{f,e} M_{HF}} \sum_{\nu=0}^{3} f_\nu \Delta H_\nu \right)}{m_{4,e}^- + m_{5,e}} \tag{78}$$

where

$$m_{4,e} \equiv \frac{M_{HF}}{M_{H_2}} Y_4 \quad \text{and} \quad m_5 \equiv \frac{M_{HF}}{M_F} Y_5 . \tag{79}$$

Formulae (77) and (78) are of a form typical of any other chemical system as long as the overall combustion can be viewed as consumption of a single fuel and single oxydizer.

2.3 Implications of the Zero Order Solutions

Insofar as the structure of the chemically active mixing zone directly affects the extraction of power, it is of interest to establish to zero order the influence exerted by Λ, diffusive transports, chemical rates and diluents upon

- o flow speed at the interface
- o location of the interface
- o flame zone mass fractions of active species
- o flame zone temperature
- o characteristic pumping lengths
- o characteristic V-T deactivation lengths

The numerical examples, except where otherwise stated, are based upon the following parameters held fixed:

$$p = 1\cdot 10^{-2}\,\text{atm},\quad u_e = 2\cdot 10^{5}\,\text{cm/sec},\quad T_e = T_{e^-} = 400^{\circ}\text{K},\quad Y_{4,e^-} = 1. \tag{80}$$

The diluents are nitrogen and helium.

The flow speed at the flame front and its location are specified by (74) which reduces to (67) for the special case of equal diffusion coefficients. A more convenient form for the velocity ratio $f'_* = u_*/u_e$ is

$$f'_* = \Lambda + \frac{Y_{4,e^-} M_F \frac{D_E}{D_I}(1-\Lambda)}{M_{N_2} Y_{5,e} + M_F Y_{4,e^-} \frac{D_{II}}{D_I}}\,. \tag{81}$$

Formula (81) implies the following. The flow speed at the flame front is the same for any combination of diluents provided their free-stream mass fractions $Y_{7,e} = 1-Y_{5,e}$ and $Y_{8,e^-} = 1-Y_{4,e^-}$

are equal and the influence of the diluents upon the diffusion coefficients is disregarded. The interface flow speed depends explicitly upon the velocity ratio Λ, relative magnitude of diffusion coefficients, and the ambient mass fractions of fuel H_2 and oxydizer F. Since $\lim_{\eta\to\infty} f' = 1$ and $\lim_{\eta\to\infty} f' = \Lambda$, values of f'_* close to 1 and Λ imply, respectively, flame front locations close to the fluorine and hydrogen streams. Inspection of (81) indicates that when $Y_{4,e-} \neq 0$ and $Y_{5,e} \to 0$, the interface attains the limiting shift towards the fluorine side and that the opposite happens when $Y_{5,e} \neq 0$ and $Y_{4,e-} \to 0$. Of course, neither limit is physically realistic because the existence of the flame front demands non-zero values of $Y_{4,e-}$ and $Y_{5,e}$. Therefore, it is worth noting that the flame does exhibit the two limiting behaviors quite well when $Y_{4,e-}$ is close to unity and $Y_{5,e}$ is small, and vice versa. The overriding control determining the location of the flame in the mixing zone is thus the relative amount of fuel and oxydizer present expressed herein in terms of the ambient mass fractions $Y_{4,e-}$ and $Y_{5,e}$; the velocity ratio Λ and the diffusion coefficients play a subservient role. The latter two quantities have the following effect: the stronger the inequality $D_{II}/D_I > 1$, the larger is the shift towards the fluorine stream and the greater the deviation from $\Lambda = 1$ the stronger is the shift towards the hydrogen stream. The physical reason for the behavior associated with $D_{II}/D_I > 1$ is that the interface stoichiometry is fixed and the more rapidly diffusing hydrogen allows for establishing the the stoichiometric mass flux ratios closer to the F-stream. The Λ influence is more complicated and depends upon the degree

of dilution of the hydrogen stream. To see this, denote formally the parametric influence upon f_*' by $f_*'(\Lambda, Y_{7,e}, Y_{8,e}, D_{II}/D_I)$. (Recall that $Y_{7,e}=1-Y_{5,e}$ and $Y_{8,e}=1-Y_{4,e-}$.) Then

$$\frac{\partial f_*'}{\partial \Lambda} = 1 - \frac{Y_{4,e-} M_F D_{II}/D_I}{M_{H_2} Y_{5,e} + Y_{4,e-} M_F D_{II}/D_I} \qquad (82)$$

Thus, when $Y_{4,e-}\to 1$ and $Y_{5,e}\to\delta_1 \ll 1$, the derivative is practically zero and becomes close to the other limiting (maximum) value 1 when $Y_{4,e-}\to\delta_2 \ll 1$ and $Y_{5,e}\to 1$. Because of the large disparity between the molecular weights of the fuel and oxydizer, the validity of the foregoing statement requires that δ_2 be substantially smaller than δ_1. In any event, the Λ-influence is much weaker in the first case than in the second. Moreover, values of $D_{II}/D_I > 1$ aid the former "limiting" behavior but hinder the latter. This is because $D_{II}/D_I > 1$ promotes a shift to the fluorine side. It may be of some practical significance to note that current parallel mixing diffusion controlled HF lasers tend to employ highly diluted F-streams interacting with pure molecular hydrogen. Now, the foregoing development indicates that in such cases manipulating velocities to promote mixing has little effect: the flame location is practically independent of Λ and always appears close to the F-stream. It is tempting to suggest that this may be one reason why, for example, the numerical results of [5,Fig.23] showing "potential power" distributions exhibit a relatively small dependence upon mixing models. A few representative values of $f_*'(\Lambda; Y_{7,e}, Y_{8,e}, D_{II}/D_I)$ are given below for $Y_{4,e-}=1$.

$D_{II}/D_I = 1,\ Y_{4,e^-} = 1$		$D_{II}/D_I = 3,\ Y_{4,e^-} = 1$	
$f_*'(0.9;0.9,0,1)$	$= 0.9990$	$f_*'(0.9;0.9,0,3)$	$= 0.9996$
$f_*'(0.5;0.9,0,1)$	$= 0.9948$	$f_*'(0.5;0.9,0,3)$	$= 0.9982$
$f_*'(0;0.9,0,1)$	$= 0.9896$	$f_*'(0;0.9,0,3)$	$= 0.9965$
$f_*'(0.9,0,0,1)$	$= 0.9905$	$f_*'(0.9;0,0,3)$	$= 0.9961$
$f_*'(0.5;0,0,1)$	$= 0.9524$	$f_*'(0.5;0,0,3)$	$= 0.9830$
$f_*'(0.5;0,0,1)$	$= 0.9524$	$f_*'(0.5;0,0,3)$	$= 0.9830$
$f_*'(0;0,0,1)$	$= 0.9048$	$f_*'(0;0,0,3)$	$= 0.9661$
$f_*'(2;0.9,0,1)$	$= 1.0104$	$f_*'(2;0.9,0,3)$	$= 1.0035$
$f_*'(2;0,0,1)$	$= 1.0952$	$f_*'(2;0,0,3)$	$= 1.0339$

The values substantiate the previous assertions. It is noted in passing that the percentage shift defined by

$$\frac{u_* - u_e}{u_{e^-} - u_e} \cdot 100 = \frac{f_*' - 1}{\Lambda - 1} \cdot 100 = \frac{Y_{5,e}\, m_{H_2}}{Y_{5,e}\, m_{H_2} + Y_{4,e^-} m_F D_{II}/D_I} \cdot 100 \qquad (83)$$

is Λ-independent. According to (83), the maximum shift is about 9.5 percent attained when $Y_{5,e}=1$ and $D_{II}/D_I=1$ and this value is reduced roughly by a factor of three when $D_{II}/D_I=3$.

At the combustion interface, mass fractions of HF_{tot}, H, and the diluents are given by

$$(Y_{HF,tot})_* = \frac{m_{HF}\, Y_{4,e^-} - Y_{5,e}}{Y_{4,e^-} m_F + Y_{5,e}\, m_{H_2}} \qquad (84)$$

$$Y_H^* = \frac{m_H\, Y_{4,e^-} - Y_{5,e}}{Y_{4,e^-} m_F + Y_{5,e}\, m_{H_2}} \qquad (85)$$

$$Y_{7,*} = Y_{7,e} \frac{M_F Y_{4,e^-}}{Y_{4,e^-} M_F + Y_{5,e} M_{H_2}} = (1 - Y_{8,e}) \frac{M_F Y_{4,e^-}}{Y_{4,e^-} M_F + Y_{5,e} M_{H_2}} \qquad (86)$$

and

$$Y_{8,*} = Y_{8,e} \frac{M_{H_2} Y_{8,e}}{Y_{4,e^-} M_F + Y_{5,e} M_{H_2}} = (1 - Y_{4,e^-}) \frac{M_{H_2} Y_{5,e}}{Y_{4,e^-} M_F + Y_{5,e} M_{H_2}} . \qquad (87)$$

The mass fractions depend only upon the prescribed ambient mass fraction values of fuel Y_{4,e^-} and oxydizer $Y_{5,e}$ and their respective molecular weights. As a consequence, it is to be expected that splitting a given amount of a single diluent between the F-stream and the H_2-stream will leave the maximum value of HF i.e.$(Y_{HF,tot})_*$ unaffected. To show this, consider the following two cases. In the first case, let the molar rates of flow of fluorine and diluent be 1:m and let the hydrogen stream be undiluted with a molar rate of flow equal to 1. Then the free stream mole fractions are $x_{5,e} = 1+m$, $x_{7,e} = m/1+m$, $x_{4,e^-} = 1$, $x_{8,e^-} = 0$. In the second case, let an amount n of the available diluent be taken away from the fluorine stream and added to the hydrogen stream. This results in new mole fractions $x_{5,e} = 1/[1+(m-n)]$ $x_{7,e} = (m-n)/[1+(m-n)]$, $x_{4,e^-} = 1/1+n$ and $x_{8,e^-} = n/1+n$. Now

$$(Y_{HF,tot})_* = \frac{M_{HF}}{\frac{M_F}{Y_{5,e}} + \frac{M_{H_2}}{Y_{4,e^-}}} = \frac{M_{HF}}{\frac{x_{5,e} M_F + [x_{Dil} M_{Dil}]_I}{x_{5,e}} + \frac{x_{4,e^-} M_{H_2} + [x_{Dil} M_{Dil}]_{II}}{x_{4,e^-}}} . \qquad (88)$$

Therefore, in case 1,

$$(Y_{HF,tot})_* = \frac{M_{HF}}{\frac{\frac{1}{1+m} M_F + \frac{m}{1+m} M_{Dil}}{\frac{1}{1+m}} + \frac{1 \cdot M_{H_2} + 0}{1}} = \frac{M_{HF}}{M_F + m M_{Dil} + M_{H_2}} \qquad (89)$$

and the same result holds in case 2. In the remainder of this subsection it is assumed that only the F-stream contains a diluent.

Zero order flame sheet temperatures (T_*°) are computed from (75) i.e.

$$\bar{H}_*^\circ = \frac{\bar{H}_{e^-} \frac{M_{HF}}{M_F} Y_{5,e} + \frac{M_{HF}}{M_{H_2}} Y_{4,e^-} + \frac{(M_{HF})^2}{M_F M_{H_2}} Y_{5,e} Y_{4,e^-} \left(\frac{1}{T_{vib,e} M_{HF}} \sum_{v=0}^{3} f_v \Delta H_v \right)}{\frac{M_{HF}}{M_{H_2}} Y_{4,e^-} + \frac{M_{HF}}{M_F} Y_{5,e}} \tag{90}$$

and

$$T_*^\circ \simeq \left[\bar{H}_*^\circ (c_{p,e} T_e + \tfrac{1}{2} u_e^2) - \tfrac{1}{2} u_*^2 \right] c_{p,*}^{-1} . \tag{91}^{9)}$$

Equation (90) indicates that the total (frozen) enthalpy ratio at the flame sheet, $\bar{H}_*^\circ$, depends upon Λ but only implicitly through $\bar{H}_{e^-}$; the explicit influence of fuel (H_2) and oxydizer (F) mass fractions and hence $Y_{7,e}$ are obvious. The temperature T_*° depends upon Λ through u_*. Because of the c_p's the temperatures depend quite strongly upon the molecular nature of the diluents.

Two sets of $\bar{H}_*^\circ$'s and hence T_*°'s are of interest. The first set is consistent with the previous development which demands $\Sigma f_v \Delta H_v = 11.79$ kcal/g-mole. In this case, the rest of the energy is taken as trapped in the vibrational levels and is potentially available for lasing. (Of course, only a fraction of this energy is actually extracted.) The second

9) In the computations, a one or two step iteration relating $c_{p,*}$ and T_*° is used. The $c_{p,*}$ is an average c_p in the sense that $\int c_p dT \simeq \bar{c}_{p,*} T_*^\circ$. In order not to clutter the notation, the bar is omitted.

set assumes a situation where no lasing takes place and all of the available energy (31.5 kcal/g-mole) ultimately appears as heat. The latter T_*°-values provide an upper bound estimate on the translational temperature. A few values of $\bar{H}_*^\circ$ and T_*° are given in the following tables.

Table 1A

Nitrogen Diluent $\sum_{v=0}^{3} f_v \Delta H_v' = 11.79$ kcal/g-mole

$\bar{H}_*^\circ(\Lambda; Y_{N_2,e})$	$=\bar{H}_*^\circ(0.9;0.9)=1.1278$;	$\bar{H}_* = 3.0709$;	$T_*^\circ=616^\circ K$
	$=\bar{H}_*^\circ(0.5;0.9)=1.1230$	$\bar{H}_{e^-}= 2.6080$;	$T_*^\circ=618^\circ K$
	$=\bar{H}_*^\circ(0.9;0) =2.1409$	$\bar{H}_{e^-}= 3.004$;	$T_*^\circ=1324^\circ K$
No diluent, pure F	$=\bar{H}_*^\circ(0.5;0) =$ ——	——	——

Table 1B

Helium Diluent $\sum_{v=0}^{3} f_v \Delta H_v = 11.79$ kcal/g-mole

$\bar{H}_*^\circ(\Lambda; Y_{He,e})$	$=H_*^\circ(0.9;0.9)=1.0749$;	$H_{e^-}= 1.8964$;	$T_*^\circ=492^\circ K$
	$=\bar{H}_*^\circ(0.5;0.9)=$ ——	——	——
	$=\bar{H}_*^\circ(0.5;0.9)=2.1409$;	$H_{e^-}= 3.004$;	$T_*^\circ=1324^\circ K$
No diluent, pure F	$=\bar{H}_*^\circ(0.5;0) =$ ——	——	——

Table 1C

Nitrogen Diluent $\sum_{v=0}^{3} f_v \Delta H_v \rightarrow$ 31.52 kcal/g-mole

$H_*^\circ(\Lambda; Y_{N_2,e})$	$= H_*^\circ(0.9;0.9)$	$= 1.3056$; $H_{e^-} = 3.0709$	T_*°	$= 926°K$
	$= H_*^\circ(0.5;09)$	$=$ ---	$=$ ---	$=$ ---
No diluent pure F	$= H_*^\circ(0.9;0)$	$= 3.7308$	$= 3.004$ T_*°	$= 2673°K$
	$= H_*^\circ(0.5;0)$	$=$ ---	$=$ ---	$=$ ---

Table 1D

Helium Diluent $\sum_{v=0}^{3} f_v \Delta H_v \rightarrow$ 31.52 kcal/g-mole

$H_*^\circ(\Lambda; Y_{He,e})$	$= H_*^\circ(0.9;0.9)$	$= 1.1847$; $H_{e^-} = 1.8964$	T_*°	$= 583°K$
	$= H_*^\circ(0.5;0.9)$	$=$ --- $H_{e^-} =$ ---		---
No diluent pure F	$= H_*^\circ(0.9;0)$	$= 3.7308$ $H_{e^-} = 3.004$	T_*°	$= 2673°K$
	$= H_*^\circ(0.5;0)$	$=$ --- $H_{e^-} =$ ---		---

The omitted entries are intended to suggest that the Λ-influence is practically nil. For the same reason, several significant figures are carried, despite the fact that the numbers themselves are at best representative of the actual physical situation. Tabulated values show that for equal free-stream mass fractions, helium keeps the flame much cooler than nitrogen.

The greatest differences resulting from substituting one diluent for another occur in the magnitudes of the

$x_{p,i}$'s and $x_{cd,i}$'s. This information is of some interest in laser design and so a few numerical values are listed. The notation $x_{p,i}(\Lambda;Y_{7,e})$ and $x_{cd,i}(\Lambda;Y_{7,e})$ is used to indicate the dependence of the chemical lengths on the parameters in the brackets. However, the Λ-effect which enters through T_*° is quite weak and for this reason only the Λ=0.9 values are given.

Table 2A

$\sum_{V=0}^{3} f_V \Delta H_V$=11.79 kcal/g-mole

M_c=20

$Sc \cdot x_{p,2}(0.9;Y_{N_2,e}=0.9) = 1.7 \cdot 10^{-3}$ cm $Sc \cdot x_{cd,2}(0.9;Y_{N_2,e}=0.9) = 9.8$ cm

$Sc \cdot x_{p,2}(0.9;Y_{He,e}=0.9) = 1.1 \cdot 10^{-2}$ cm $Sc \cdot x_{cd,2}(0.9;Y_{He,e}=0.9) = 58$ cm

Table 2B

$\sum_{V=0}^{3} f_V \Delta H_V$=31.52 kcal/g-mole

M_c=20

$Sc \cdot x_{p,2}(0.9;Y_{N_2,e}=0.9) = 1.6 \cdot 10^{-3}$ cm $Sc \cdot x_{cd,2}(0.9;Y_{N_2,2}=0.9) = 8.6$cm

$Sc \cdot x_{p,2}(0.9;Y_{He,e}=0.9) = 1 \cdot 10^{-2}$ cm $Sc \cdot x_{cd,2}(0.9;Y_{He,e}=0.9) = 55$cm

Table 2C

$\sum_{V=0}^{3} f_V \Delta H_V$=11.79 kcal/g-mole (pure F-stream)

M_c=20

$Sc \cdot x_{cd,2} = Sc \cdot x_{cd,2}(0.9;0) = 1.96$ cm

Table 2D

$$\sum_{v=0}^{3} f_v \Delta H_v \rightarrow 31.52 \text{ kcal/g-mole (pure F-stream)}$$

$$M_c = 20$$

$$S_c \cdot x_{cd,2} = Sc \cdot x_{cd,2}(0.9;0) = 1.59\text{cm}$$

The foregoing tabulations are based upon the formulae

$$Sc \cdot x_{p,2} = \frac{u_e}{2} \frac{1}{a_2'} \frac{m_{H_2}}{Y_{4,e}} \frac{m_F}{Y_{5,e}} \frac{Y_{2,*}^{\circ}}{m_{HF}} \cdot \frac{1}{\rho_*^{\circ}} e^{c/T_*^{\circ}} \tag{92}$$

and

$$Sc \cdot x_{cd,2} = \frac{u_e}{2} \frac{1}{a_5} \frac{1}{(T_*^{\circ})^b} \frac{m_c}{Y_{c,*}^{\circ}} \frac{1}{\rho_*^{\circ}} \tag{93}$$

Tables 2A-2D indicate that on a mass basis helium acts as a better collisional deactivation buffer than nitrogen. For comparable conditions, the $x_{cd,i}$'s are evidently stretched by about a factor of 6 when helium is substituted for nitrogen. There is a corresponding stretch of the x_p's. While this is undesirable, the x_p's are small enough and so the stretching of the x_{cd}'s is of the greater practical significance.

Comparison of Table 2A with the value given in 2C indicates clearly the significant role played by either one of the diluents. It is observed that if no diluent were used, $x_{cd,2}$ would shrink by about a factor of 29 for the helium case and approximately by a factor of 5 for the nitrogen case. The high degree of dilution was taken to exemplify some extremes. Of course, the

absolute values of $Sc \cdot x_{cd,2}$'s are in quite some doubt but the relative values, expressed as ratios, should be much better. The absolute values are sensitive to $M_C/Y^\circ_{C,*}$. Those given in the last column are based upon $M_C=20$ which means that the influence of atomic hydrogen is neglected and HF – in whatever energy state – is assumed to act as the sole collisional deactivator. This assumption is very likely poor. Certainly, when no diluent is present (either one of the last two cases)

$$\left(Y^\circ_{HF,tot}\right)_* + Y^\circ_{H,*} = 1 \,, \qquad Y^\circ_{H,*} = \frac{1}{20}\left(Y^\circ_{HF,tot}\right)_* . \tag{94}$$

Hence, $(Y^\circ_{HF,tot})_* = 0.952$ and $Y^\circ_{H,*} = 0.048$. If it is now assumed that H and HF are equally efficient deactivators, then

$$\frac{1}{M_c} = \left[\frac{1}{20}\left(Y^\circ_{HF,tot}\right)_*\right] + Y^\circ_{H,*}$$

$$M_c = 10.5 \tag{95}$$

and

$$\frac{M_c}{Y^\circ_{C,*}} = \frac{10.5}{\left(Y^\circ_{HF,tot}\right)_* + Y^\circ_{H,*}} = 10.5$$

Consequently, the entries in Tables 2C and 2D are roughly halved. In these circumstances, the collisional deactivation length $Sc \cdot x_{cd,2}$ collapses to a few millimeters. While then the boundary layer as well as the flame sheet concepts are suspect, the illustrative example nevertheless retains

considerable force in showing the crucial role played by the diluents. An identical decrease takes place when either one of the diluents is present, providing one argues as follows. Let H and HF be equally active and let the buffer gas leave M_c unaffected. As an example, consider the helium case which gave $Sc \cdot x_{cd,2} = 58cm$. For this case $[Y^{\circ}_{HF,tot}]_* = 0.1042$ and $Y_{H,*} = 0.0052$ and the sum is 0.1094. Defining $[\hat{Y}^{\circ}_{HF,tot}]_* \equiv 0.1042/0.1094 = 0.952$ and $\hat{Y}^{\circ}_{H} \equiv 0.0052/0.1094 = 0.048$ and repeating (95) in terms of these values yields the same result.

Because the molecular weights of helium and nitrogen differ by a factor of 7, it is pertinent to compare the effectiveness of the two diluents on a mole basis. It suffices to consider one case only. Let $\Lambda = 0.9; Y_{F,e} = 0.1$ and $Y_{N_2,e} = 0.9$. The corresponding free-stream mole fractions are $X_{F,e} = 0.1337$ and $X_{N_2,e} = 0.8593$. The pertinent case for comparison is thus $X_{F,e} = 0.1337$, $X_{He} = 0.8593$ or equivalently $Y_{F,e} = 0.425$ and $Y_{He,e} = 0.575$. The following are the results:

$$f'_*(0.9; 0.575) = 0.9957; \left(Y^{\circ}_{HF,tot}\right)_* = 0.4282, \; Y^{\circ}_{He,*} = 0.5504$$

$$Y^{\circ}_{H,*} = 0.0214; \; H_{e^-} = 2.187, \; \bar{H}^{\circ}_* = 1.362, \; T^{\circ}_* = 665^{\circ}K \qquad (96)$$

$$Sc\, x_{p,2} = 7.1 \cdot 10^{-3}\, cm \text{ and } Sc\, x_{cd,2} = 10; \; M_c = 20.$$

It is seen that now $Sc \cdot x_{p,2}$ and $Sc \cdot x_{cd,2}$ are roughly comparable to the nitrogen case in Table 2A. However, the helium diluent admits a fourfold increase in $(Y^{\circ}_{HF,tot})_*$ – the maximum HF mass fraction – and so, on this basis too, helium is preferable to nitrogen.

It remains to remark on some practical aspects of the flame sheet model and to outline the rationale for applying the former to the nozzle configuration (Fig.2). The criteria are based upon magnitudes of the pumping and collisional deactivation Damkohler numbers. Because all diffusion equations are handled in the same manner, the discussion is again confined to the Y_2 -diffusion equation.

In a strict sense, the flame sheet model is valid for min $\zeta_p \to \infty$. However, practical experience with the type of combustion problems discussed here, [7] and [8], suggests that the flame front is reasonably well developed for ζ_p's on the order of 100. To get an idea of the actual lengths involved, consider the nitrogen case of Table 2A. Now,

$$\frac{\zeta_{p,2}}{\zeta_{p,2}=1} = 100 = \frac{x}{x_p} = \frac{x}{1.7\cdot10^{-3}} \quad , \tag{97}$$

yields x = 0.17cm. On this basis, the flame front begins to assert itself quite closely to the initial point of contact between the H_2 and F-streams. At x = 0.17cm, $\zeta_{cd,2}/(\zeta_{cd,2}=1) = x/x_{cd} \approx 0.17/5 = 0.034$ where the lower value of $M_C/Y^{\circ}_{C,*}$ was used to indicate the effect of atomic hydrogen. If it is assumed that the power series in ζ_{cd} (given in the next section) are valid say up to $\zeta_{cd,2} = 0.4$ then this translates to an applicable x-range on the order of 2cm. The latter value is within the lasing zone range of the diffusion limited HF lasers now operating and, from this point of view, the flame front model is of practical significance. It is interesting to note that in

the cited example, the ratio

$$\frac{\zeta_{p,2}}{\zeta_{cd,2}} = \frac{a_2' \frac{Y_{4,e}}{m_{H_2}} \frac{Y_{5,e}}{m_F} \frac{m_{HF}}{Y^o_{3,e}}}{a_5 (T^o_*)^b \frac{Y^o_{5,H}}{m_c}} \qquad (98)$$

which exceeds 10^3 has a minimum at $T^o_* = c/b \approx 660°R$. At this temperature, $x_{cd,2}/x_{p,2}$ has a maximum. The latter is quite flat and tends to suggest the desirability of low free-stream temperatures.

Unlike the semi-infinite stream configuration, the nozzle geometry (Fig. 2) possesses an inherent length scale: the F-nozzle height d. Thus, in order for the flame sheet model to be of practical value, not only must the foregoing discussion apply but also one additional criterion must be met: the flame zone thickness must be small in comparison to d, say an order of magnitude less than d. A crude estimate of the flame zone thickness is the chemical pumping length x_p. A few values of x_p were given in Tables 2A and 2B. On this basis it follows that the flame sheet model is valid for F-nozzles as small as a few millimeters. For nozzles still smaller, the flow tends to remain frozen in the core flow regime and perhaps somewhat further downstream as well. Consequently, the H_2 and F-streams undergo substantial mixing before any significant chemical interactions take place. The one dimensional pre-mixed flow model discussed by J. Skifstad [3] is then appropriate.

2.4 The Perturbation Equations

Three types of perturbations ought to be mentioned. The first two are connected with the primary pumping reactions and from the physical standpoint are related to flame sheet broadening. This occurs when either the $\zeta_{p,i}$'s are finite and backward pumping Damkohler numbers are zero or when $\zeta_{p,i} \to \infty$ and backward pumping Damkohler numbers are non-zero.[10] In both cases, the perturbation problems are singular and of the type discussed in [7] and [8].

This study is concerned with perturbations of the third kind which are regular and arise when $\zeta_{p,i} \to \infty$, $(\zeta_{p,i})_{\text{backward reaction}} \equiv 0, \max \zeta_{cd,i} < 1$. The situation is the following. A flame-sheet flow field is established (zero order problem) and small changes in its structure caused by collisional deactivation are evaluated through appropriate series in powers of collisional deactivation Damkohler numbers. The flame sheet itself remains a surface of discontinuity. No broadening takes place.

Herein, the variables which reflect the action of collisional deactivation are the three Damkohler numbers, $\zeta_{cd,3}$, $\zeta_{cd,2}$ and $\zeta_{cd,1}$. It is convenient to relabel these:

$$\xi_1 \equiv \zeta_{cd,3}\,, \quad \xi_2 \equiv \zeta_{cd,2} \quad \text{and} \quad \xi_3 \equiv \zeta_{cd,1}\,. \tag{99}$$

Each of the foregoing variables influences $Y_{HF,v}$ and therefore the general series for Y^i (previously written as Y_i) where i = 0, 1, 2 and 3 is of the form

$$\begin{aligned} Y^i = {} & Y^i_{000} + Y^i_{100}\xi_1 + Y^i_{010}\xi_2 + Y^i_{001}\xi_3 + Y^i_{200}\xi_1^2 + Y^i_{020}\xi_2^2 \\ & + Y^i_{002}\xi_3^2 + Y^i_{110}\xi_1\xi_2 + Y^i_{101}\xi_1\xi_3 + Y^i_{011}\xi_2\xi_3 + \cdots \end{aligned} \tag{100}$$

[10] Backward pumping Damkohler numbers are those based upon the backward reactions 0-4 in (5).

The set of perturbation equations is obtained by first substituting the normalized version of (100),

$$\bar{Y}^i_{\varepsilon} \equiv \frac{Y^i}{\bar{Y}^i_{\varepsilon,0}} = \bar{Y}^i_{000} + \bar{Y}^i_{100}\xi_1 + \bar{Y}^i_{010}\xi_2 + \bar{Y}^i_{001}\xi_3 + \cdots \qquad (101)$$

into the corresponding set of diffusion equations expressed in the s,η variables, collecting then powers and products of the ζ's and finally, reading off the coefficient set of the differential equations. The latter are the perturbation equations. For example: substituting (101) with i = 3 into (34) gives

$$\begin{aligned}
&\Big(\bar{Y}^3_{000} + \bar{Y}^3_{100}\xi_1 + \bar{Y}^3_{010}\xi_2 + \bar{Y}^3_{001}\xi_3 + \bar{Y}^3_{200}\xi_1^2 + \bar{Y}^3_{020}\xi_2^2 \\
&\quad + \bar{Y}^3_{002}\xi_3^2 + \bar{Y}^3_{110}\xi_1\xi_2 + \bar{Y}^3_{101}\xi_1\xi_3 + \bar{Y}^3_{001}\xi_2\xi_3\Big)'' \\
&+ Scf\Big(\bar{Y}^3_{000} + \bar{Y}^3_{100}\xi_1 + \bar{Y}^3_{010}\xi_2 + \bar{Y}^3_{001}\xi_3 + \bar{Y}^3_{200}\xi_1^2 \\
&\quad + \bar{Y}^3_{020}\xi_2^2 + \bar{Y}^3_{002}\xi_3^2 + \bar{Y}^3_{110}\xi_1\xi_2 + \bar{Y}^3_{101}\xi_1\xi_3 + \bar{Y}^3_{011}\xi_2\xi_3\Big)' \\
&- Sc\,\xi_1\Big(\frac{T}{T_\infty}\Big)^{\beta}\frac{\rho}{\rho_\infty}\bar{Y}_e\Big(\bar{Y}^3_{000} + \bar{Y}^3_{100}\xi_1 + \bar{Y}^3_{010}\xi_2 + \bar{Y}^3_{001}\xi_3 \qquad (102) \\
&\quad + \bar{Y}^3_{200}\xi_1^2 + \bar{Y}^3_{020}\xi_2^2 + \bar{Y}^3_{002}\xi_3^2 + \bar{Y}^3_{110}\xi_1\xi_2 + \bar{Y}^3_{101}\xi_1\xi_3 + \bar{Y}^3_{200}\xi_2\xi_3\Big) \\
&= 2Scf'\Big(0 + \bar{Y}^3_{100}\xi_1 + \bar{Y}^3_{010}\xi_2 + \bar{Y}^3_{001}\xi_3 + 2\bar{Y}^3_{200}\xi_1^2 \\
&\quad + 2\bar{Y}^3_{020}\xi_2^2 + 2\bar{Y}^3_{002}\xi_3^2 + 2\bar{Y}^3_{110}\xi_1\xi_3 + 2\bar{Y}^3_{101}\xi_1\xi_3 + 2\bar{Y}^3_{011}\xi_2\xi_3\Big)
\end{aligned}$$

where the ' denotes differentiation with respect to η and where each $\bar{Y}^3_{ijk}$ is a function of η alone. Equation (102) utilizes the fact that f is a function only of η and that each derivative with respect to the streamwise variable s can be expressed in terms of any ζ_i, = 1, 2 and 3. Now, since the first term in the square bracket of (102) contains ten terms, (102) generates ten differential equations for $\bar{Y}^3_{ijk}$. This set is the following:

Level v=3

0-term: $$\bar{Y}^{3\,\prime\prime}_{000} + Scf\,\bar{Y}^{3\,\prime}_{000} = 0$$

ζ_1-term: $$\bar{Y}^{3\,\prime\prime}_{100} + Scf\,\bar{Y}^{3\,\prime}_{100} - 2Scf'\bar{Y}^{3}_{100} = Sc\left(\frac{T}{T_*}\right)^b \frac{\rho}{\rho_*}\bar{Y}_c\,\bar{Y}^{3}_{000}$$

ζ_2-term: $$\bar{Y}^{3\,\prime\prime}_{010} + Scf\,\bar{Y}^{3\,\prime}_{010} - 2Scf'\bar{Y}^{3}_{010} = 0$$

ζ_3-term: $$\bar{Y}^{3\,\prime\prime}_{001} + Scf\,\bar{Y}^{3\,\prime}_{001} - 2Scf'\bar{Y}^{3}_{001} = 0$$

$\zeta_1\zeta_2$-term: $$\bar{Y}^{3\,\prime\prime}_{110} + Scf\,\bar{Y}^{3\,\prime}_{110} - 4Scf'\bar{Y}^{3}_{110} = Sc\left(\frac{T}{T_*}\right)^b \frac{\rho}{\rho_*}\bar{Y}_c\,\bar{Y}^{3}_{010} \qquad (103)$$

$\zeta_1\zeta_3$-term: $$\bar{Y}^{3\,\prime\prime}_{101} + Scf\,\bar{Y}^{3\,\prime}_{101} - 4Scf'\bar{Y}^{3}_{101} = Sc\left(\frac{T}{T_*}\right)^b \frac{\rho}{\rho_*}\bar{Y}_c\,\bar{Y}^{3}_{001}$$

$\zeta_2\zeta_3$-term: $$\bar{Y}^{3\,\prime\prime}_{011} + Scf\,\bar{Y}^{3\,\prime}_{011} - 4Scf'\bar{Y}^{3}_{011} = 0$$

ζ_1^2-term: $$\bar{Y}^{3\,\prime\prime}_{200} + Scf\,\bar{Y}^{3\,\prime}_{200} - 4Scf'\bar{Y}^{3}_{200} = Sc\left(\frac{T}{T_*}\right)^b \frac{\rho}{\rho_*}\bar{Y}_c\,\bar{Y}^{3}_{100}$$

ζ_2^2-term: $$\bar{Y}^{3\,\prime\prime}_{020} + Scf\,\bar{Y}^{3\,\prime}_{020} - 4Scf'\bar{Y}^{3}_{020} = 0$$

ζ_3^2-term: $$\bar{Y}^{3\,\prime\prime}_{002} + Scf\,\bar{Y}^{3\,\prime}_{002} - 4Scf'\bar{Y}^{3}_{002} = 0$$

Clearly, $(103)_1$ is the prototype of the equations generating the zero order solutions discussed previously. All other equations are perturbation equations up to order ζ^2. Only $(103)_1$, $(103)_2$ and $(103)_6$ possess non-trivial solutions; the rest of the system (103) reduces to identities, i.e., the remaining equations have the trivial solutions.

$$\bar{Y}^3_{010} = \bar{Y}^3_{001} = \cdots = \bar{Y}^3_{002} = 0. \tag{104}$$

The statement (104) is a consequence of the fact that each perturbation equation must satisfy homogeneous zero-boundary conditions at $+\infty$ and $-\infty$. Therefore, for example, the solution to the homogeneous equation $(103)_5$ is $\bar{Y}^3_{010} \equiv 0$. Taking cognizance of this fact, equation $(103)_5$ is really homogeneous also. Thus $\bar{Y}^3_{100} \equiv 0$ and so on. All other non-trivial perturbation equations generated by the $\bar{Y}_2$ and $\bar{Y}_1$ diffusion equations are obtained by analogous arguments and by noting certain structural identities among the equations. The results are as follows:

Level v=2

$$\text{0-term:} \quad \bar{Y}^{2\,\prime\prime}_{000} + Sc\, f\, \bar{Y}^{2\,\prime}_{000} = 0$$

$$\zeta_1\text{- term:} \quad \bar{Y}^2_{100} = -\bar{Y}^3_{100}\, \bar{Y}^0_{3,\infty} / \bar{Y}^0_{2,\infty}$$

$$\zeta_2\text{- term:} \quad \bar{Y}^{2\,\prime\prime}_{010} + Sc\, f\, \bar{Y}^{2\,\prime}_{010} - 2\, Sc\, f'\, \bar{Y}^2_{010} = Sc \left(\frac{T}{T^0_\infty}\right)^b \frac{\rho}{\rho^0_\infty}\, \bar{Y}_e\, \bar{Y}^2_{000} \tag{105}$$

$$\zeta_1^2\text{- term:} \quad \bar{Y}^{2\,\prime\prime}_{200} = -\bar{Y}^3_{200}\, \bar{Y}^0_{3,\infty} / \bar{Y}^0_{2,\infty}$$

$$\zeta_2^2\text{- term:} \quad \bar{Y}^{2\,\prime\prime}_{020} + Sc\, f\, \bar{Y}^{2\,\prime}_{020} - 4\, Sc\, f'\, \bar{Y}^2_{020} = Sc \left(\frac{T}{T^0_\infty}\right)^b \frac{\rho}{\rho^0_\infty}\, \bar{Y}_e\, \bar{Y}^2_{010}$$

$$\zeta_1\zeta_2\text{ - term:} \quad \bar{Y}^{2\,\prime\prime}_{110} + Sc\, f\, \bar{Y}^{2\,\prime}_{110} - 4\, Sc\, f'\, \bar{Y}^2_{110} = Sc \left(\frac{T}{T^0_\infty}\right)^b \frac{\rho}{\rho^0_\infty}\, \bar{Y}_e\, \bar{Y}^2_{100}$$

Level v = 1

0 -term: $$\bar{Y}^1_{000} + Scf\,\bar{Y}^{1\prime}_{000} = 0$$

ζ_2-term: $$\bar{Y}^1_{010} = -\bar{Y}^2_{010}\,\bar{Y}^0_{2,*}/\bar{Y}^0_{1,*}$$

ζ_3-term: $$\bar{Y}^{1\prime\prime}_{001} + Scf\,\bar{Y}^{1\prime}_{001} - 4Scf'\bar{Y}^1_{001} = Sc\left(\frac{T}{T^0_*}\right)^b \frac{\rho}{\rho^0_*}\bar{Y}_c\bar{Y}^1_{000} \qquad (106)$$

ζ_2^2-term: $$\bar{Y}^1_{020} = -\bar{Y}^2_{020}\,\bar{Y}^0_{2,*}/\bar{Y}^0_{1,*}$$

ζ_3^2-term: $$\bar{Y}^{1\prime\prime}_{002} + Scf\,\bar{Y}^{1\prime}_{002} - 4Scf'\bar{Y}^1_{002} = Sc\left(\frac{T}{T^0_*}\right)^b \frac{\rho}{\rho^0_*}\bar{Y}_c\bar{Y}^1_{001}$$

$\zeta_2\zeta_3$-term: $$\bar{Y}^{1\prime\prime}_{011} + Scf\,\bar{Y}^{1\prime}_{011} - 4Scf'\bar{Y}^1_{011} = Sc\left(\frac{T}{T^0_*}\right)^b \frac{\rho}{\rho^0_*}\bar{Y}_c\bar{Y}^1_{010}$$

Level v = 0

0 -term: $$\bar{Y}^{0\prime\prime}_{000} + Scf\,\bar{Y}^{0\prime}_{000} = 0$$

ζ_3-term: $$\bar{Y}^0_{001} = -\bar{Y}^1_{001}\,\bar{Y}^0_{1,*}/\bar{Y}^0_{0,*} \qquad (107)$$

ζ_3^2-term: $$\bar{Y}^0_{002} = -\bar{Y}^1_{002}\,\bar{Y}^0_{1,*}/\bar{Y}^0_{0,*}$$

$\zeta_2\zeta_3$-term: $$\bar{Y}^0_{011} = -\bar{Y}^1_{011}\,\bar{Y}^0_{1,*}/\bar{Y}^0_{0,*}$$

Each of the foregoing perturbation equations may be solved in two parts satisfying the boundary conditions

$$\bar{Y}^{i\prime}_{ijk}(\eta_*)=0\ ,\quad \lim_{\eta\to\infty}\bar{Y}^{i}_{ijk}(\eta)=0\ ,\quad +\infty>\eta\geq\eta_*\ ;$$
$$\bar{Y}^{i\prime}_{ijk}(\eta_*)=0\quad \lim_{\eta\to-\infty}\bar{Y}^{i}_{ijk}(\eta)=0\quad -\infty<\eta\leq\eta_*\ . \tag{108}$$

The derivatives are zero at η_* because the zero order terms by themselves satisfy the required mass balance at the interface. It is worth noting that collisional deactivation is distributed throughout the mixing layer, that no sources or sinks exist anywhere, and that in particular the derivatives of the perturbation variables are continuous at the interface which is the location of maximum $Y_{HF,v}$'s.

The explicit forms of the perturbation series (101) are the following:

$$\bar{Y}^3=\bar{Y}^3_{000}+\bar{Y}^3_{100}\xi_1+0\cdot\xi_2+0\cdot\xi_3+\bar{Y}^3_{200}\xi_1^2$$
$$+0\cdot\xi_2^2+0\cdot\xi_3^2+0\cdot\xi_1\xi_2+0\cdot\xi_1\xi_3+0\cdot\xi_2\xi_3+\cdots; \tag{109}$$

$$\bar{Y}^2=\bar{Y}^2_{000}-\bar{Y}^3_{100}\frac{\bar{Y}^0_{3,*}}{\bar{Y}^0_{2,*}}\xi_1+\bar{Y}^2_{010}\xi_2+0\cdot\xi_3-\bar{Y}^3_{200}\frac{\bar{Y}^0_{3,*}}{\bar{Y}^0_{2,*}}\xi_1^2$$
$$+\bar{Y}^2_{020}\xi_2^2+0\cdot\xi_3^2+\bar{Y}^2_{110}\xi_1\xi_2+0\cdot\xi_1\xi_3+0\cdot\xi_2\xi_3+\cdots; \tag{110}$$

$$\bar{Y}^1 = \bar{Y}^1_{000} + 0\cdot\xi_1 - \bar{Y}^2_{010}\,\frac{Y^0_{2,*}}{Y^0_{1,*}}\,\xi_2 + \bar{Y}^1_{001}\,\xi_3 + 0\cdot\xi_1^2$$
$$- \bar{Y}^2_{020}\,\frac{Y^0_{2,*}}{Y^0_{2,*}}\,\xi_2^2 + \bar{Y}^1_{002}\,\xi_3^2 - \bar{Y}^2_{110}\,\frac{Y^0_{2,*}}{Y^0_{1,*}}\,\xi_1\xi_2 + 0\cdot\xi_1\xi_3 + \bar{Y}^1_{011}\,\xi_2\xi_3 + \cdots; \tag{111}$$

and

$$\bar{Y}^0 = \bar{Y}^0_{000} + \xi_1\cdot 0 + 0\cdot\xi_2 - \bar{Y}^1_{001}\,\frac{Y^0_{1,*}}{Y^0_{0,*}}\,\xi_3 + 0\cdot\xi_1^2 + 0\cdot\xi_2^2$$
$$- \bar{Y}^1_{002}\,\frac{Y^0_{1,*}}{Y^0_{0,*}}\,\xi_3^2 + 0\cdot\xi_1\xi_2 + 0\cdot\xi_1\xi_3 - \bar{Y}^1_{011}\,\frac{Y^0_{1,*}}{Y^0_{0,*}}\,\xi_2\xi_3 + \cdots. \tag{112}$$

The corresponding set of Y^i's follows from the definition (101).

A few observations are worthwhile. There is a one-to-one correspondence between the summability properties of the two sets of perturbation expansions and the generating set of diffusion equations whose prototypes are (33) and (34). This correspondence is the following. Upon summing the unnormalized differential equations for Y^3, Y^2, Y^1 and Y^0, one obtains the differential equation for $Y_{HF,tot}$ in the s,η variables; the analogous property of the unbarred Y^i series implied by (110)-(112) is that

$$\sum_{i=0}^{3} Y^i = Y_{HF,tot}\,. \tag{113}$$

The second correspondence is obtained by comparing

$$\sum_{i=0}^{3} \bar{Y}^i \neq \bar{Y}_{HF,tot} \equiv Y_{HF,tot}/(Y_{HF,tot})_* \tag{114}$$

with the sum of the differential equations of the type (34).

This sum does not reproduce the differential equation for for $\bar{Y}_{HF,tot}$. The statement (113) demands that all perturbation terms sum to zero identically and may be viewed as a compatibility condition dictating the particular forms of the expansions used in this report.[11] In turn, the summability properties just mentioned imply that the diffusion field itself possesses a dual structure. For large primary pumping rates it is similar (in the boundary layer sense) with respect to the overall production of HF. Now, in view of the global reaction $H_2+F \rightarrow HF_{tot}+H$, similarity exists for the H_2, H and F species and also for the diluents. In contrast, the set of mass fractions HF(v) forms a substructure that in the zeroth approximation belongs to the similarity class but not otherwise. This substructure is imbedded into the overall field in a very specific way reflected in the summability properties. It is this duality which distinguishes the current perturbation problems from numerous others discussed in [7]. It is noted in passing that the point of view adopted by Hofland and Mirels in [1] (apparently the only other paper on the subject related to this section) appears to be incompatible with the approach taken herein. One tends to suspect that conclusions based upon solutions of the perturbation equations presented in this report may be different from those of [1].

The mathematics of the perturbation scheme reflects the physical nature of the chemical model that may be summarized as follows. Because deactivation proceeds only downward and and in single steps, each intermediate level (i.e. levels one or two) is affected solely by its immediate higher neighbor

---

11) In fact, one may take (113) as the starting point and then deduce the appropriate ζ_{cd}-expansions. The approach taken herein is more direct and guarantees that (113) is automatically satisfied.

and in turn affects only its adjacent lower neighbor. In other words, up to order of ζ^2, each such level takes no direct cognizance of any level other than its immediate partners. The situation is pictured in the following diagram:

	(a)	(b)	(c)	(d)
$\nu = 3$ ———	ζ_1;	Y^3;	ζ_1, ζ_1^2	
$\nu = 2$ ———	ζ_2;	Y^2;	ζ_1, ζ_2;	ζ_1^2, ζ_2^2 and $\zeta_1\zeta_2$
$\nu = 1$ ———	ζ_3;	Y^1;	ζ_2, ζ_3;	ζ_2^2, ζ_3^2 and $\zeta_2\zeta_3$
$\nu = 0$ ———		Y^0;	ζ_3,	ζ_3^2, and $\zeta_2\zeta_3$

Columns (a) and (b) underscore the notation by showing the Damkohler numbers and mass fractions associated with the levels given on the left. Columns (c) and (d) exhibit respectively the Damkohler numbers appearing in each expansion up to orders ζ and ζ^2. The coupling is reflected in the "cross terms," namely the products $\zeta_1\zeta_2$ and $\zeta_2\zeta_3$. Note the special nature of the top and ground levels in accord with the previous statements.

Since no solutions to the perturbation problems are presented in this report, it is appropriate to make the following closing remarks. The system consisting of $(103)_2$, $(103)_8$, $(105)_{2\text{-}6}$, $(106)_{2\text{-}4}$, and $(107)_{2\text{-}4}$ is less formidable than it appears at first glance. To a good approximation, the right hand sides can be simplified by setting $Sc(T/T_*^\circ)^b(\rho/\rho_*^\circ)$ equal to a constant. This procedure decouples the diffusion equations from the energy equation and is consistent with the treatment of the zero order problem presented earlier. The mass fraction Y_C is obtained from the zero order

solutions and therefore always belongs to the similarity class. This means that all of the linear perturbation equations can be solved sequentially. Finally, it is emphasized that while no closed form solutions are available, numerical solutions are quite simple. What is more important, such solutions can be obtained once and for all and, because of the structure of the expansions, do not detract from the explicit nature of the results.

2.5 Radiation

The influence of radiation upon the flow manifests itself through the appearance of additional source terms in the diffusion equations for HF(v) and the energy equation and by the appearance of the radiative transfer equation. This general set written in terms of local optical gain is given, for example, in [2] and [4]. Herein, attention is focused on the high power case which is of main practical interest. With regard to the flame front model, the foregoing situation implies radiation fields of sufficient intensity so that radiative deactivation takes place at the site of formation of the active species, i.e., the flame sheet. The medium is transparent elsewhere. In these circumstances,the radiative transfer equation is effectively bypassed and the energy equation is affected through the interface energy balance. To obtain the resultant distribution of active species and hence power, it suffices to consider the diffusion equations alone.[12)]

In connection with the high-power model, two diametrically opposed assumptions are evidently employed. The first is typified by Skifstad [3] who assumes that rotational equilibrium holds irrespective of the magnitude of intensity. The second is exemplified by the work of Hofland and Mirels [2] who abandon the equilibrium hypothesis. Practical considerations make it worthwhile to examine assumptions made in [2] and [3].

[12)] It is noted that because the new mass source terms appear in the diffusion equations for HF(v) and no others, the direct effect is to alter the distribution of the excited species alone. Couplings of the conservation equations through physical and transport properties exert a secondary influence which is in part accounted for through the similarity transformations. Thus, radiation is viewed as mainly influencing the detailed chemical structure through the HF(v)'s but otherwise as leaving the global structure of the flow unaltered.

The intent here parallels that of Section 2.1. Once again, the governing differential equations expressed in the s,η variables are used to generate a set of dimensionless parameters that characterize the influence exerted by the radiation field (in terms of energy density or intensity) upon the detailed chemical structure of the flow. Because each such parameter is an analogue of the ζ's, it is called a radiative Damkohler number. In carrying out this plan, there arise certain practical difficulties even though no such difficulties exist in principle. To see the reasons for this, it is best to re-emphasize the approach taken earlier with radiation effects excluded: 1) the hierarchy of governing boundary layer equations was used to yield a set of characteristic parameters; 2) the relative magnitude of these parameters dictated in turn permissible mathematical simplifications of the equations themselves. On this basis, the validity of the diffusion limited flame sheet model was not assumed a priori but instead was deduced from the general equations as a consequence of the magnitudes of the various Damkohler numbers. Because collisional deactivation involved v-levels but not the rotational states within them, it was sufficient to regard the mixture as one containing chemically distinct active species HF(0), HF(1), HF(2) and HF(3) without explicit regard of the various rotational states.

Radiative transitions involve rotational states within the v-levels. This means that if the procedure outlined in the previous sections were actually followed, it would be necessary to enlarge the ensemble of the active species to include the rotational states within each v (i.e. to consider HF(v;j) j=0, 1...) and thus to include rotational kinetics. If this were done, comparison of the hierarchy of radiative

Damkohler numbers with those generated by considerations of rotational kinetics would dictate under what conditions the assumption of rotational equilibrium is permissible and under what conditions it must be abandoned. This procedure cannot be followed in this report. Nevertheless, it is possible to deal with the question of rotational equilibrium, however crudely, within the framework of the equations given here and without explicit regard of rotational kinetics. The results presented in the latter part of this section show that the assumption of rotational equilibrium, while obviously permissible for the "small power" case, is in some doubt for high intensity fields.

At this point, it is convenient to employ substantially the same notation as well as the main concepts presented recently by Skifstad [3]. A few modifications are introduced wherever required by the more general flow model employed in this report.[13] The prototype of the diffusion equations expressed in the x,y variables is that governing $Y_2 \equiv Y_{HF(2)} \equiv Y_{HF,2}$:

$$\rho u \frac{\partial Y_{HF,2}}{\partial x} + \rho v \frac{\partial Y_{HF,2}}{\partial y} = \frac{\partial}{\partial y}\left(\rho D \frac{\partial Y_{HF,2}}{\partial y}\right) + \rho^2 k_{f,2} \frac{Y_{H_2}}{m_{H_2}} \frac{Y_F}{m_F} m_{HF}$$

$$+ \rho^2 k_{f,4} \frac{Y_{HF,3}}{m_{HF}} \frac{Y_C}{m_C} m_{HF} - \rho^2 k_{f,5} \frac{Y_{HF,2}}{m_{HF}} \frac{Y_C}{m_C} m_{HF} + \rho u_{y;3,2} B_{3,2} Y_{HF,3,j_3} \quad (115)$$

$$+ \rho u_{y;1,2} B_{1,2} Y_{HF,1,j_2+1} - \rho u_{y;2,1} B_{2,1} Y_{HF,2,j_2} - \rho u_{y;2,3} B_{2,3} Y_{HF,2,j_3+1}.$$

---

[13] Skifstad prefers to consider the indirect problem in that he specifies line intensities (or energy densities) in the lasing region rather than the combination of optical path length through the medium and mirror reflectivities. His choice of energy density distributions allows for discussing the implications of the radiative transfer equation separately from flow and kinetics.

In (115), the last four terms account for radiation; namely, stimulated emission from the adjacent higher level v=3; absorption from the next lower level v=1; stimulated emission from v=2; and absorption from v=2. While the various terms are given in the Nomenclature, it is useful to note here that u_ν stands for the spectral energy density and that B_{lu} denotes the transition probability for induced emission related to the transition probability for spontaneous emission A_{ul} through

$$B_{lu} = \frac{g_u}{g_l} \frac{c^3}{8\pi h \nu^3} A_{ul}. \tag{116}$$

The subscripts l and u stand for "lower" and "upper" levels respectively and g denotes degeneracy. Only P-branch transitions are considered and therefore the degeneracies satisfy

$$\frac{g_{v-1}}{g_v} = \frac{2j_v + 3}{2j_v + 1} \tag{117}$$

and

$$\frac{g_v}{g_{v+1}} = \frac{2j_{v+1} + 3}{2j_{v+1} + 1} \tag{118}$$

where j_v refers to the rotational quantum number of the upper level of transition. Stimulated emissions are due to transitions $v, j_v \rightarrow v-1, j_v+1$ and absorption is associated with the transitions $v-1, j_v+1 \rightarrow v, j_v$. The transition probabilities B_{lu} and B_{ul} are related as follows:

$$B_{ul} = \frac{g_l}{g_u} B_{lu}. \tag{119}$$

Incorporating (117)-(119) into (115) yields

$$\rho u \frac{\partial Y_{HF,2}}{\partial x} + \rho v \frac{\partial Y_{HF,2}}{\partial y} = \frac{\partial}{\partial y}\left(\rho D \frac{\partial Y_{HF,2}}{\partial y}\right) + \rho^2 k_{f,2} \frac{Y_{H_2} Y_F}{M_{H_2} M_F}$$

$$+ \rho^2 k_{f,4} \frac{Y_{HF,3}}{M_{HF}} \frac{Y_C}{M_C} M_{HF} - \rho^2 k_{f,5} \frac{Y_{HF,2}}{M_{HF}} \frac{Y_C}{M_C} + \rho u_{v;3,2} \frac{2j_3+3}{2j_3+1} B_{2,3} Y_{HF,3,j_3} \tag{120}$$

$$+ \rho u_{v,1,2} B_{1,2} Y_{HF,1,j_2+1} - \rho u_{v,2,1} \frac{2j_2+3}{2j_2+1} B_{1,2} Y_{HF,2,j_2} - \rho u_{v,2,3} B_{2,3} Y_{HF,2,j_3+1}.$$

From (115) or (120) it is evident that further progress requires relationships connecting the mass fractions Y_{HF,v,j_v} to $Y_{HF,v}$. For the moment (and mainly for the purpose of estimating the magnitudes of radiative Damkohler numbers), it will suffice to assume rotational equilibrium as was done in [3] and elsewhere. Later, the situation is re-examined in light of a specific nonequilibrium model. The rotational equilibrium assumption amounts to saying that rotational relaxation rates are much higher than other competing rates and that the population of the rotational levels may therefore be taken to be in equilibrium at the translational temperature of the gas.

Let l_v^+ and l_v^- denote the fractions of the population in the vibrational level v corresponding, respectively, to the lower level of the transition $v+1, j_{v+1} \to v, j_{v+1}+1$ and the upper level of the transition $v, j_v \to v-1, j_v+1$. This means that

$$Y_{HF,v,j_{v+1}+1} = l_v^+ Y_{HF,v} \tag{121}$$

and

$$Y_{HF,v;j_v} = l_v^- Y_{HF,v}. \tag{122}$$

Now, in accord with assuming equilibrium, it follows that

$$l_v^+ = (2j_{v+1}+3)\frac{\Theta_R}{T}\exp\left[-(j_{v+1}+1)(j_{v+1}+2)\frac{\Theta_R}{T}\right] \tag{123}$$

and

$$l_v^- = (2j_v+1)\frac{\Theta_R}{T}\exp\left[-j_v(j_v+1)\frac{\Theta_R}{T}\right] \tag{124}$$

where the rotational partition function is approximated by the usual integral which equals T/θ_R. For the HF molecule, the characteristic rotational temperature $\theta_R = 30.15°K$.

Equation (120) may be expressed as

$$\begin{aligned}
&\rho u\frac{\partial Y_{HF,2}}{\partial x} + \rho v\frac{\partial Y_{HF,2}}{\partial y} = \frac{\partial}{\partial y}\left(\rho D\frac{\partial Y_{HF,2}}{\partial y}\right) + \rho^2 k_{f,2}\frac{Y_{H_2}}{M_{H_2}}\frac{Y_F}{M_F} \\
&+ \rho^2 k_{f,4}\frac{Y_{HF,3}}{M_{HF}}\frac{Y_c}{M_c}M_{HF} - \rho^2 k_{f,5}\frac{Y_{HF,2}}{M_{HF}}\frac{Y_c}{M_c} \\
&+ \rho u_{v;2,3}\frac{\Theta_R}{T}B_{2,3}(2j_3+1)e^{-(j_3+1)(j_3+2)\frac{\Theta_R}{T}}\left(Y_{HF,3}e^{2\frac{\Theta_R}{T}(j_3+1)} - Y_{HF,2}\right) \\
&- \rho u_{v;1,2}\frac{\Theta_R}{T}B_{1,2}(2j_2+3)e^{-(j_2+1)(j_2+2)\frac{\Theta_R}{T}}\left(Y_{HF,2}e^{2\frac{\Theta_R}{T}(j_2+1)} - Y_{HF,1}\right)
\end{aligned} \tag{125}$$

and this equation, under the transormation $x,y \to s,\bar{\eta} \to s,\eta$ takes the form

$$\begin{aligned}
&\frac{\partial}{\partial\eta}\left(\frac{\partial Y_{HF,2}}{\partial\eta}\right) + Sc\,f\frac{\partial Y_{HF,2}}{\partial\eta} + Sc\frac{2x}{u_e}\rho k_{f,2}\frac{Y_{H_2}}{M_{H_2}}\frac{Y_F}{M_F} \\
&+ Sc\frac{2x}{u_e}\rho k_{f,4}\frac{Y_{HF,3}}{M_{HF}}\frac{Y_c}{M_c}M_{HF} - Sc\frac{2x}{u_e}\rho k_{f,5}\frac{Y_{HF,2}}{M_{HF}}\frac{Y_c}{M_c} \\
&+ Sc\frac{2x}{u_e}u_{v;2,3}\frac{\Theta_R}{T}B_{2,3}(2j_3+3)e^{-(j_3+1)(j_3+2)\frac{\Theta_R}{T}}\left(Y_{HF,3}e^{2\frac{\Theta_R}{T}(j_3+1)} - Y_{HF,2}\right) \\
&- Sc\frac{2x}{u_e}u_{v;1,2}\frac{\Theta_R}{T}B_{1,2}(2j+3)e^{-(j_2+1)(j_2+2)\frac{\Theta_R}{T}}\left(Y_{HF,2}e^{2\frac{\Theta_R}{T}(j_2+1)} - Y_{HF,2}\right) = 2Sc\cdot s\left(\frac{\partial Y_{HF,2}}{\partial s}\frac{\partial f}{\partial\eta} - \frac{\partial f}{\partial s}\frac{\partial Y_{HF,2}}{\partial\eta}\right).
\end{aligned} \tag{126}$$

Now, to obtain the prototypes of radiative Damkohler numbers, an anologue of (36) is required. In non-dimensionalizing the radiative terms, it is convenient once again to adopt a procedure similar to that used by Skifstad [3]. He puts

$$u_{\nu;\nu-1,\nu} = u_\nu^\circ \lambda_\nu F(\theta) \tag{127}$$

and introduces a reference value for the transition probabilities, B_{ref}, through

$$B_{\nu-1,\nu} = \beta_\nu B_{ref}. \tag{128}$$

In (127), u_ν° is a constant value of the spectral energy density and λ_ν where $\nu=1$, 2 and 3 is taken as a distribution function for the intensity levels of the lines such that

$$\sum_{\nu=1}^{3} \lambda_\nu = 1. \tag{129}$$

The coefficients β_ν are on the order of unity or slightly larger. In order to obtain closed form solutions, Skifstad [3] chooses $F(\theta)$ to equal a certain density ratio. A different choice is appropriate here, namely,

$$u_{\nu;\nu-1,\nu} = u_\nu^\circ \lambda_\nu \rho_*^\circ/\rho \tag{130}$$

where ρ_*° is the reference density associated with the zero order solution given earlier. [14] The analogue of (36) incorporating (128) and (130) is obtained from (126) and the result is

---

[14] Skifstad adopts (127) in order to decouple all of the diffusion equations from the energy equation. Herein, (130) parallels his (127) in intent in that a ρT product (subsequently approximated by a constant) appears in the s,η transformed diffusion equations. But, in the case of the flame sheet model for a medium near saturation, the choice (130) is not as important as in [3]; in the current limiting situation, the radiative terms behave like the chemical pumping terms and hence do not explicitly enter the final governing equation. It is also worth noting that Skifstad, in assuming different forms of (127), found no drastic changes in his results.

$$(\bar{Y}_{HF,2})_{\eta\eta} + Sc\, f(\bar{Y}_{HF,2})_{\eta} + Sc\left(\frac{2x}{u_e}\rho_*^\circ a_2' \frac{Y_{4,e}^\circ}{M_{H_2}} \frac{Y_{F,e}^\circ}{M_F} \frac{M_{HF}}{Y_{2,*}^\circ}\right)\frac{\rho}{\rho_*^\circ} e^{-\frac{\xi}{T_*^\circ}\left(\frac{1}{\theta}-1\right)} \bar{Y}_{H_2}\bar{Y}_F$$

$$+ Sc\left[\frac{2x}{u_e}\rho_*^\circ (T_*^\circ)^b a_4 \frac{Y_{3,*}^\circ}{M_{HF}} \frac{Y_{e,*}^\circ}{M_e} M_{HF} \frac{1}{Y_{2,*}^\circ}\right]\frac{\rho}{\rho_*^\circ}\left(\frac{T}{T_*^\circ}\right)^b \bar{Y}_{HF,3}\bar{Y}_e$$

$$- Sc\left[\frac{2x}{u_e}\rho_*^\circ (T_*^\circ)^b a_5 \frac{1}{M_{HF}} \frac{Y_{e,*}^\circ}{M_e} M_{HF}\right]\frac{\rho}{\rho_*^\circ}\left(\frac{T}{T_*^\circ}\right)^b \bar{Y}_{HF,2}\bar{Y}_e \qquad (131)$$

$$+ Sc\left[\frac{2x}{u_e} u_\nu^\circ \lambda_3\beta_3 B_{ref}\right]\frac{\Theta_R}{T_*^\circ}\cdot\frac{\rho_*^\circ T_*^\circ}{\rho T}(2j_3+3)e^{-(j_3+2)(j_3+2)\frac{\Theta_R}{T_*^\circ}\cdot\frac{1}{\theta}}\left(\bar{Y}_{HF,3}e^{\frac{2}{\theta}\frac{\Theta_R}{T_*^\circ}(j_3+1)} Y_{H_2,3,*}^\circ - \bar{Y}_{HF,2}\right)$$

$$- Sc\left[\frac{2x}{u_e} u_\nu^\circ \lambda_2\beta_2 B_{ref}\right]\frac{\Theta_R}{T_*^\circ}\cdot\frac{\rho_*^\circ T_*^\circ}{\rho T}(2j_2+3)e^{-(j_2+1)(j_2+2)\frac{\Theta_R}{T_*^\circ}\frac{1}{\theta}}\left(\bar{Y}_{HF,2}e^{\frac{2}{\theta}\frac{\Theta_R}{T_*^\circ}(j_2+1)} - \bar{Y}_{HF,1}\, Y_{H_2,1,*}^\circ\right) = 2Sc\cdot s\left[f_\eta(\bar{Y}_{HF,2})_s - f_s(\bar{Y}_{HF,2})_\eta\right].$$

The radiative Damkohler numbers are now identified with the groups of terms in the square brackets containing u_ν°, that is,

$$\zeta_{r,3} \equiv \zeta_{r;2,3} \equiv \frac{2x}{u_e} u_\nu^\circ (\lambda_3\beta_3) B_{ref} \qquad (132)$$

and

$$\zeta_{r,2} \equiv \zeta_{r;2,2} = \frac{2x}{u_e} u_\nu^\circ (\lambda_2\beta_2) B_{ref} \qquad (133)$$

The first is associated with the line connecting levels two and three and the second corresponds to the line connecting levels one and two.

From the definitions (132) and (133), it follows that values of the radiative Damkohler numbers span a range encompassing those comparable in magnitude to the $\zeta_{cd,i}$'s as well as those comparable to or exceeding the $\zeta_{p,i}$'s. It is easy to show that the first situation defines what is usually called the "small power" case and that the second case occurs near saturation conditions. Which of the two extremes prevails depends on the magnitude of u_ν°.

Attention is now focussed on the radiative deactivation length scales $x_{rd,i}$ implied by (132) and (133). A relative comparison of the $x_{rd,i}$'s with the $x_{cd,i}$'s and $x_{p,i}$'s is sought and therefore each $x_{rd,i}$ is obtained by setting its corresponding $\zeta_{rd,i}$ equal to unity. For example:

$$x_{rd;1\to 2} \equiv x_{rd,2} = \frac{u_e}{2} \frac{1}{u_\nu^\circ(\lambda_2\beta_2) B_{ref}} \tag{134}$$

At this point, it is convenient to relate the energy densities to line radiancies. Skifstad's development [3, Laser Parameters] is applicable and thus

$$u_\nu = 2\left(\frac{\ln 2}{\pi}\right)^{1/2} \frac{\langle R_L \rangle}{c b_D} \tag{135}$$

where

$$b_D = \left(2 \frac{\ln 2 kT}{mc^2}\right)^{1/2} \nu_{ul} \tag{136}$$

is the Doppler half-width of a line. The reader is referred to [3] for further details. In view of (135) and (136), it follows that

$$x_{rd;2} = \frac{u_e}{2} \frac{1}{(\beta_2\lambda_2) B_{ref}} \cdot \frac{1}{2}\left(\frac{\pi}{\ln 2}\right)^{1/2} \frac{c b_D}{\langle R_L \rangle_2} \tag{137}$$

For illustrative purposes, it is better not to assign values to $\langle R_L \rangle$ but instead to assign values to the $x_{rd,i}$'s and inquire about the corresponding magnitudes of line radiancies. First, suppose $x_{rd,2}$ is on the order of $x_{cd,2}$. Then, for the conditions given in Section 2.1 (highly diluted F-stream, cool flame) $x_{cd,2}$ is on the order of 10 centimeters. Taking again $T_*^\circ \simeq 600°K, p_e = p_{e-} = 1 \cdot 10^{-2} atm, u_e = 2 \cdot 10^5 cm/sec$, $Y_{N_2,e} = 0.9$ and $x_{cd,2} \simeq 10$ cm gives

$$\langle R_L \rangle_2 = \frac{u_e}{2} \frac{1}{(\beta_2 \lambda_2) B_{ref}} \frac{1}{2} \left(\frac{\pi}{\ln 2} \right)^{1/2} \frac{c b_D}{x_{rd,2}} \simeq 0.07 \frac{w}{cm^2} . \qquad (138)$$

This value is based upon $\beta_2 = 1.23$, $\lambda_2 = 1/3$, $B_{ref} = 2.538 \cdot 10^{17}$ and $\nu_{21} = 1.07 \cdot 10^{14}$ taken from [3] and the HF-output spectrum of [9]. Second, suppose that $x_{rd,2}$ is on the order of the corresponding pumping length $x_{p,2}$. Under the same ambient conditions, the latter value is on the order $1.7 \cdot 10^{-3}$cm. Therefore, the corresponding $\langle R_L \rangle_2$ is given by

$$\langle R_L \rangle_2 = \frac{u_e}{2} \frac{1}{(\beta_2 \lambda_2) B_{ref}} \frac{1}{2} \left(\frac{\pi}{\ln 2} \right)^{1/2} \frac{c b_D}{x_{p,2}} \simeq 4 \cdot 10^2 \frac{w}{cm^2} . \qquad (139)$$

The foregoing estimates are rough because the quantities entering the radiative Damkohler numbers are somewhat arbitrary. Nonetheless, the values of the line radiancies just given ought to delineate the regime of radiative deactivation within an order of magnitude. In the first case, radiative deactivation, like its collisional counterpart, takes place in the entire mixing layer. In the second example, deactivation occurs at the flame front itself.

Finally, suppose that a typical time for rotational equilibrium is an order of 10^{-2} seconds smaller than the

characteristic pumping time. In steady flow, consider therefore a corresponding length scale smaller than $x_{p,2}$ by a factor of 10^{-2} cm. In this case

$$\langle R_L \rangle_2 = \frac{u_e}{2} \frac{1}{(\beta_2 \lambda_2) B_{ref}} \cdot \frac{1}{2} \left(\frac{\Pi}{\ell n 2} \right) \frac{c b_D}{x_{p,2} \cdot 10^{-2}} \simeq 4 \cdot 10^4 \frac{W}{cm^2} . \qquad (140)$$

On this basis, it appears that rotational relaxation effects ought to arise under the stated conditions when $\langle R_L \rangle_2 > 4 \cdot 10^4 \frac{W}{cm^2}$. For the flame sheet model, the last estimate is rather artificial in that the structure of the flame sheet itself must come into play. Despite this, the example is highly suggestive, implying that the usual equilibrium assumption is likely to be questionable for high power devices. It is worth noting that in most theoretical works on chemical lasers, the rotational equilibrium assumption is retained irrespective of the magnitude of intensities.

A few additional comments are pertinent. First, the question is raised as to the degree of confidence one is to attach to the foregoing estimates in view of the fact that they are based upon equations which contain the assumption of rotational equilibrium to begin with. In this respect, it is noted that the equilibrium assumption enters only into the fractions 1_v^+ and 1_v^- as given by (123) and (124). Clearly, (121) and (122) remain valid; it is only necessary to provide new fractions 1_v^+ and 1_v^- that do not depend upon the equilibrium assumption. Such alternate estimates can be obtained. For the conditions cited previously, the new 1_v^+'s appear to be within a factor of four or so of the equilibrium 1_v^+'s when the j_v's are in the range of four

to eight. This tends to suggest that the estimates given in the foregoing paragraphs are likely to be reasonable. The procedure for obtaining alternate l_v's is outlined below.

In all major respects, the ideas are the same as those employed by Hofland and Mirels [2] who claim validity for their model at saturation. To aid the reader in obtaining further details, the notation of [2] is left intact. It is assumed that excited HF-molecules are still initially distributed in the various v-levels in accord with the pumping reactions (5) and that all rotational states are given by the equilibrium distribution. Therefore, prior to lasing,

$$\frac{n_{v,j}}{n_v} = \frac{2j+1}{q_R(v)} e^{-\alpha_v j(j+1)} \qquad j = 0, 1, \ldots \tag{141}$$

where

$$q_R(v) \equiv \sum_{j=0}^{\infty} (2j+1) e^{-\alpha_v j(j+1)}$$

is the rotational partition function, $\alpha_v \equiv \Theta_R(v)/T$, $\Theta_R(v)$ is the characteristic rotational temperature for level v, and n_v denotes the number of molecules per unit volume in the vibrational level v. As in [2], it is further assumed that both the 2/1 and 1/0 vibrational bands are initially totally inverted but that $n_3 << n_2$. Consideration is given to P-branch sharp-line lasing transitions in the high-power limit.

The central new assumption is that the population inversion is destroyed completely by reducing the gain

to zero on all possible P-branch transitions. This assumption allows for obtaining the total number of photons released as well as the final vibration-rotation distribution in terms of the initial $n_{v,j}$'s (or n_v's). The physical implication is that a molecule undergoing a transition has no means of communicating the event to its neighbors; rotational equilibrium no longer holds. This situation is quite different from that embodied in the assumptions (123) and (124) and reflected further in the prototypes of the diffusion equations (125), (126) and (131). Consequently, while in both instances one is concerned with the case $\min \zeta_{rd,i} \to \infty$, the chemical compositions of the flows are different. It is convenient to indicate the reason for this here and at the same time establish a point of contact between the "high power" limiting case based upon the equilibrium assumption and the Hofland-Mirels case. It suffices to note that terms in each of the diffusion equations (125), (126) and (131) may be written in terms of products of gain and intensity. The integrated gain for the transition $v, j_v \to v-1, j_v+1$ is

$$\hat{a}_v = h N_A \left(\frac{m}{2\pi k}\right)^{1/2} \frac{f}{\bar{m}_{HF}} \beta_v B_{ref} \frac{\Theta_R}{T} (2j_v+3) e^{(j_v+1)(j_v+2)\frac{\Theta_R}{T}} \left(Y_{HF,v} e^{2(j_v+1)\frac{\Theta_R}{T}} - Y_{HF,v-1}\right). \quad (142)$$

Because the radiative terms in the diffusion equations must remain bounded, it follows, for example, from (131), (132) and (133) that as $\zeta_{r,3} \to \infty$ the gain necessarily goes to zero and hence

$$\left(Y_{HF,3} e^{2(j_3+1)\frac{\Theta_R}{T}} - Y_{HF,2}\right) \to 0. \quad (143)$$

More generally, at saturation under the equilibrium assumption,

$$(\gamma_{HF,v})_{sat}\, e^{2(j_v+1)\frac{\Theta_R}{T}} = (\gamma_{HF,v-1})_{sat}\,. \tag{144}$$

The distribution embodied in (144) is to be contrasted with that obtained under the Hofland-Mirels assumption. The procedure is indicated in the next few paragraphs.

Let now n' and n" denote the number of molecules per unit volume after lasing; n' is connected with the destruction of the population inversion on the 1/0 band and n" refers to the final distribution after taking into account the influence of the second vibrational level. Under the rotational non-equilibrium assumption of [2], it is possible to treat the deactivation of the first vibrational level as an independent event.[15] It is desired to obtain the final distributions $n''_{v,j}/n''_v$, n''_v and, in passing, the total number of photons released, all in terms of the given initial distributions.

The zero gain condition for the P-branch transition implies that stimulated emission balances absorption and therefore

$$\frac{n'_{v,j+1}}{[2(j+1)+1]} = \frac{n'_{v-1,j+2}}{[2(j+2)+1]} \tag{145}$$

Of course, (145) also holds for the " variables. On physical grounds it follows that

$$(n_{1,0} - n'_{1,0}) + (n_{1,1} - n'_{1,1}) + \cdots = (n'_{0,1} - n_{0,1}) + (n'_{0,2} - n_{0,2}) + \cdots \tag{146}$$

---

[15] The reader may wish to consult Patel's paper [10] in which he discusses non-equilibrium effects in a qualitative way.

The generic term of the foregoing series is written as

$$\Delta_{10,j} \equiv n_{1,j+1} - n'_{1,j+1} = n'_{0,j+2} - n_{0,j+2} \tag{147}$$

and the total number of photons released from v=1 alone is the sum

$$\sum_{j=-1}^{\infty} \Delta_{10,j} . \tag{148}$$

The reader may wish to note that in (146) term-by-term equalities of the type

$$n_{1,0} - n'_{1,0} = n'_{0,1} - n_{0,1} \tag{149}$$

hold and that the sum (148) starts with j=-1 since no P-branch transition from v=1 can terminate on j=0 in v=0. All this is consistent with the foregoing discussion in the sense that each molecule leaving level v=1 and arriving in level v=0 is fixed in its terminal state without communication with its neighboring molecules. The zero gain condition (145) is now combined with (147) to yield

$$n_{1,j+1} - n'_{1,j-1} = \frac{2j+5}{2j+3} n'_{2,j+1} - n_{0,j+2} \tag{150}$$

whence it follows that

$$n'_{1,j+1} = \frac{2j+3}{4j+8} \left(n_{1,j+1} - n_{0,j+2} \right). \tag{151}$$

In view of (151), the generic term (147) may be expressed as

$$\Delta_{10,j} = n_{1,j+1} - n'_{1,j+1} = \frac{1}{4j+8}\left[(2j+5)n_{1,j+1} - (2j+3)n_{0,j+2}\right] \qquad (152)$$

where the initial $n_{v,j}$'s are given by (141) i.e.,

$$n_{1,j+1} = \frac{2(j+1)+1}{q_R(1)}\, e^{-d_1(j+1)(j+2)}$$

and

$$n_{0,j+2} = \frac{2(j+2)+1}{q_R(0)}\, e^{-d_0(j+2)(j+3)}.$$

The total number of photons released in deactivating v=1 is therefore

$$\sum_{j=-1}^{\infty} \Delta_{10,j} = \sum_{j=-1}^{\infty} \frac{1}{4j+8}\left[(2j+5)\, n_{1,j+1} - (2j+3)n_{0,j+2}\right]. \qquad (153)$$

Clearly,

$$n'_1 = \sum_{j=-1}^{\infty} n'_{1,j+1} \qquad (154)$$

whence by (151) and (154) the intermediate distributions $n'_{1,j+1}/n'_1$ are easily obtained. These are omitted because only the final " distributions which take into account the influence of v=2 are of interest.

Consider now the number of molecules in states v,j after cancellation of the population inversion among the three states (v,j), (v-1, j+1) and (v-2,j+2). Let

$$\Delta_{21,j} \equiv n''_{1,j+1} - n'_{1,j+1} \tag{155}$$

and

$$\Delta_{20,j} \equiv n''_{0,j+2} - n'_{0,j+2} \tag{156}$$

denote respectively the number of molecules undergoing transitions from v=2 to v=1 and from v=2 to v=0. (The latter transitions constitute a departure from those considered under the equilibrium assumption.) Once again, the zero gain condition gives

$$n''_{1,j+1} = \frac{2j+3}{2j+5}\, n''_{0,j+2} \tag{157}$$

and

$$n'_{1,j+1} = \frac{2j+3}{2j+5}\, n'_{0,j+2}\,. \tag{158}$$

In view of (157) and (158), $\Delta_{21,j}$ and $\Delta_{20,j}$ are related by

$$\Delta_{20,j} = \frac{2j+5}{2j+3}\, \Delta_{21,j}\,. \tag{159}$$

A second relationship connecting $\Delta_{21,j}$ and $\Delta_{20,j}$ is obtained on physical grounds:

$$\Delta_{21,j} + \Delta_{20,j} = n_{2,j} - n''_{2,j} \tag{160}$$

which states that the total number of photons released in the transition from v=2 equals the difference between the initial and final number of molecules (per unit volume) for each j. From the definition (155) and (151), (159)

and (160), it follows now that

$$\Delta_{21,j}\,\frac{6j+9}{2j+3} = n_{2,j} - \frac{2j+1}{4j+8}\left(n_{1,j+1} + n_{0,j+2}\right) \tag{161}$$

and in terms of the initial n_ν's, the result (161) is

$$\Delta_{21,j} = \tfrac{1}{3}(2j+1)\Big[\frac{1}{q_R(2)}\,e^{-\alpha_2(j+1)j}\,n_2 - \frac{1}{4j+8}\Big(\frac{2j+3}{q_R(3)}\,e^{-\alpha_1(j+1)(j+2)}\,n_1 + \frac{2j+5}{q_R(0)}\,e^{-\alpha_0(j+2)(j+3)}\,n_0\Big)\Big]. \tag{162}$$

The quantity $\Delta_{20,j}$ is given in terms of the initial distribution by (162) and (159). The total number of photons released as a result of all interactions,

$$\Delta_{10,-1} + \sum_{j=0}^{\infty}\left(\Delta_{10,j} + \Delta_{21,j} + 2\Delta_{20,j}\right) \tag{163}$$

may be expressed in the form

$$\Delta_{10,-1} + \sum_{j=0}^{\infty}\left(\Delta_{10,j} + \Delta_{21,j} + 2\Delta_{20,j}\right)$$

$$= \frac{3}{4}\frac{1}{q_R(1)}\,n_1 + \frac{1}{4}\frac{3}{q_R(0)}\,e^{-2\alpha_0}\,n_0 + \sum_{j=0}^{\infty}\Big[\frac{(6j+13)(2j+1)}{3(2j+3)}\,\frac{e^{-\alpha_2 j(j+1)}}{q_R(2)}\,n_2 + \frac{4}{3}\,e^{-\alpha_1(j+1)(j+2)}\,\frac{1}{q_R(1)}\,n_1 + \frac{(6j+5)(2j+5)}{3(2j+3)}\,e^{-\alpha_0(j+2)(j+3)}\,\frac{n_0}{q_R(0)}\Big]. \tag{164}$$

In (163) the factor 2 arises because each jump from 2→0 is associated with the release of two photons.

The final v,j distributions in the form n''_{vj}/n''_v can now be determined. It is convenient to give the foregoing ratios in terms of the fractions

$$Z_v = \frac{n''_v}{\sum_{v=0}^{3} n''_v} . \tag{165}$$

The latter are analoques of the initial fractions

$$Z_v = \frac{n_v}{\sum_{v=0}^{3} n_v} = \frac{\gamma_{HF,v}}{\gamma_{HF,tot}} = \frac{k_{f,v}}{\sum_{v=0}^{3} k_{f,v}} \tag{166}$$

where $k_{f,v}$ stands for the rates of the pumping reactions. Consider first the level v=0. Since no P-branch transition from the upper levels can terminate on j=0, it follows that

$$n''_{0,0} = n_{0,0} = \frac{n_0}{q_R(0)} \tag{167}$$

Therefore,

$$\frac{n''_{0,0}}{n''_0} = \frac{n_0}{n''_0}\frac{1}{q_R(0)} = \frac{n_0}{\sum_{v=0}^{3} n_v}\frac{\sum_{v=0}^{3} n''_v}{n''_0}\frac{1}{q_R(0)} \tag{168}$$

and upon introducing the ratios (165) and (166) there results

$$\frac{n''_{0,0}}{n''_0} = Z_0 \frac{1}{q_R(0)} \frac{1}{Z_0} \tag{169}$$

In a similar fashion one obtains

$$\frac{n''_{0,1}}{n''_0} = \frac{n_{0,1} + \Delta_{10,-1}}{n''_0} = \frac{1}{Z_0}\left(\frac{3}{4}\frac{z_1}{q_R(1)} + \frac{9}{4}\frac{z_0}{q_R(0)}e^{-2d_0}\right) \tag{170}$$

The general term for v=0

$$\frac{n''_{0,j+2}}{n''_0} = \frac{1}{Z_0}\left[\frac{(2j+5)^2}{3(2j+3)}\frac{1}{q_R(0)}e^{-d_0(j+2)(j+3)}z_0\right. \tag{171}$$

$$\left. + \frac{2j+5}{2j+3}\frac{1}{q_R(1)}e^{-d_1(j+1)(j+2)}z_1 + \frac{(2j+5)(2j+1)}{3(2j+3)}\frac{1}{q_R(2)}e^{-d_2(j+1)j}z_2\right.$$

is obtained from

$$n''_{0,j+2} = \Delta_{20,j} + n'_{0,j+2} = \Delta_{20,j} + n_{0,j+2} + \Delta_{10,j}$$

which is valid for j=0, 1,..... The unknown Z_0 is determined by solving

$$\frac{n''_{0,0}}{n''_0} + \frac{n''_{0,1}}{n''_0} + \frac{\sum_{j=0}^{\infty} n''_{0,j+2}}{n''_0} = 1 \tag{172}$$

for Z_0 resulting in the expression

$$Z_0 = \frac{1}{q_R(0)}\left[1 + \frac{9}{4}e^{-2d_0} + \sum_{j=0}^{\infty}\frac{(2j+5)^2}{3(2j+3)}e^{-d_0(j+2)(j+3)}\right. \tag{173}$$

$$\left. + \frac{1}{q_R(1)}\left[\frac{3}{4} + \sum_{j=0}^{\infty}\frac{2j+5}{2j+3}e^{-d_1(j+1)(j+2)}\right]z_1 + \frac{1}{q_R(2)}\left[\sum_{j=0}^{\infty}\frac{(2j+5)(2j+1)}{(2j+3)3}e^{-d_2 j(j+1)}\right]z_2.\right.$$

The same type of procedure is applied to levels v=1 and v=2. The pertinent results may be summarized as follows:

$$\frac{n''_{1,0}}{n''_1} = \frac{1}{Z_1}\left[\frac{1}{4}\frac{1}{q_R(1)} Z_1 + \frac{3}{4}\frac{1}{q_R(0)} e^{-2d_0} Z_0\right] ; \tag{174}$$

$$\frac{n''_{1,j+1}}{n''_1} = \frac{1}{Z_1}\left[\frac{1}{q_R(2)}\frac{2j+1}{3} e^{-d_2 j(j+1)} Z_2 + \frac{1}{q_R(1)}\frac{2j+3}{3} e^{-d_1(j+1)(j+2)} Z_1\right. \tag{175}$$

$$\left. + \frac{2j+5}{3}\frac{1}{q_R(0)} e^{-d_0(j+2)(j+3)} Z_0\right] , \quad j=0,1,\cdots j$$

$$Z_1 = \frac{1}{q_R(0)}\left[\frac{3}{4} e^{-2d_0} + \sum_{j=0}^{\infty}\frac{2j+5}{3} e^{-d_0(j+2)(j+3)}\right] Z_0 \tag{176}$$

$$+ \frac{1}{q_R(1)}\left[\frac{1}{4} + \sum_{j=0}^{\infty}\frac{2j+3}{3} e^{-d_1(j+1)(j+2)}\right] Z_1 + \frac{1}{3} Z_2 ;$$

$$\frac{n''_{2,j}}{n''_2} = \frac{1}{Z_2}\left[\frac{(2j+1)^2}{3(2j+3)}\frac{1}{q_R(2)} e^{-d_2 j(j+1)} Z_2 + \frac{2j+1}{3}\frac{1}{q_R(1)} e^{-d_1(j+1)(j+2)} Z_1\right. \tag{177}$$

$$\left. + \frac{(2j+1)(2j+5)}{3(2j+3)}\frac{1}{q_R(0)} e^{-d_0(j+2)(j+3)} Z_0\right] , \quad j=0,1,\cdots ;$$

$$Z_2 = \frac{1}{q_R(0)}\left[\sum_{j=0}^{\infty}\frac{(2j+1)(2j+5)}{3(2j+3)}e^{-d_0(j+2)(j+3)}\right]Z_0$$

$$+\frac{1}{q_R(1)}\left[\sum_{j=0}^{\infty}\frac{(2j+1)}{3}e^{-d_1(j+1)(j+2)}\right]Z_1 + \frac{1}{q_R(2)}\left[\sum_{j=0}^{\infty}\frac{(2j+1)^2}{3(2j+3)}e^{-d_2 j(j+1)}\right]Z_2 \qquad (178)$$

The foregoing vibration-rotation distributions are to be contrasted with those based upon the equilibrium assumption given in equations (121)-(124). Since a ratio such as (175) also equals a corresponding ratio of mass fractions, a formal definition of the new l_v's can be given. This procedure is not convenient for computations because of the appearance of the infinite series in the z_v's. However, the latter were evaluated in [2] in a sufficiently wide range of temperatures. For conditions close enough to those taken under the equilibrium assumption, the shift from the Boltzmann distribution implies the factor of 4 or so change in the equilibrium l_v's mentioned elsewhere in the report.

It appears then that a rough estimate of the rotational nonequilibrium effects can be obtained by comparing the distribution of active species at saturation under the equilibrium assumption and under the assumption of [2]. Corresponding assessment of power output is then accessible with the aid of formulae given in [2, Sect.III, B] and [3, Laser Parameters].

2.6 Closing Comment

The report provides a basis for a sufficiently general theory of HF lasers operating in the diffusion limited regime. regime.

Potential power output and its degradation as a result of collisional deactivation can be assessed from the zero order solutions and the boundary value problems based upon the perturbation equations given in Section 2.4. Computational effort in connection with the perturbation equation system describing collisional deactivation should prove to be minimal and yield useful new results. Some care is evidently called for in handling rotational non-equilibrium effects that are likely to arise near saturation.

REFERENCES

1. Hofland, R., and Mirels, H., "Flame Sheet Analysis of C.W. Diffusion-Type Chemical Lasers," AIAA Paper No. 71-28, 9th Aerospace Sciences Meeting, New York, 1971.

2. Hofland, R., and Mirels, H., "Flame Sheet Analysis of C.W. Diffusion-Type Chemical Lasers: Coupled Radiation," Aerospace Report No. TR-0172(2240-01)-3, May 1972.

3. Skifstad, J. G., "Theory of an HF Chemical Laser," Combustion Science and Technology, Vol. 6, pp. 287-306, 1973.

4. King, W.S., Mirels, H., "Numerical Study of a Diffusion Type Chemical Laser," AIAA Paper No. 72-146, 10th Aerospace Sciences Meeting, San Diego, 1972.

5. Thoenes, J., Ratliff, A.W., and Benefield, J.W., "Analytical Program for Continuous Wave Chemical Laser Device," Report No. RK-TR-71-19, U. S. Army Missile Command, Redstone Arsenal, Alabama, 1971.

6. Hayday, A.A., "Some Aspects of the Cavity Flow Problem of an HF Chemical Laser," SCICOM Report No. RR-103, 1973.

7. Chung, P.M., "Chemically Reacting Nonequilibrium Boundary Layers," Advances in Heat Transfer, Vol.2, Academic Press, New York-London, 1965.

8. Chung, P.M., Fendell, F.E., and Holt, J.F., "Non-equilibrium Anomalies in the Development of Diffusion Flames," AIAA Journal, Vol. 4, No. 6, pp. 1020-1026, 1966.

9. Spencer, D.J., Mirels, H., and Durran, D.A., "Performance C.W. HF Chemical Laser with N_2 or He Diluent." Aerospace Report No. TR-0172(2777)-1, March 1972.

10. Patel, C.K.N, "Gas Lasers," Lasers Vol. 2, Marcel Dekker, Inc., New York, 1968.

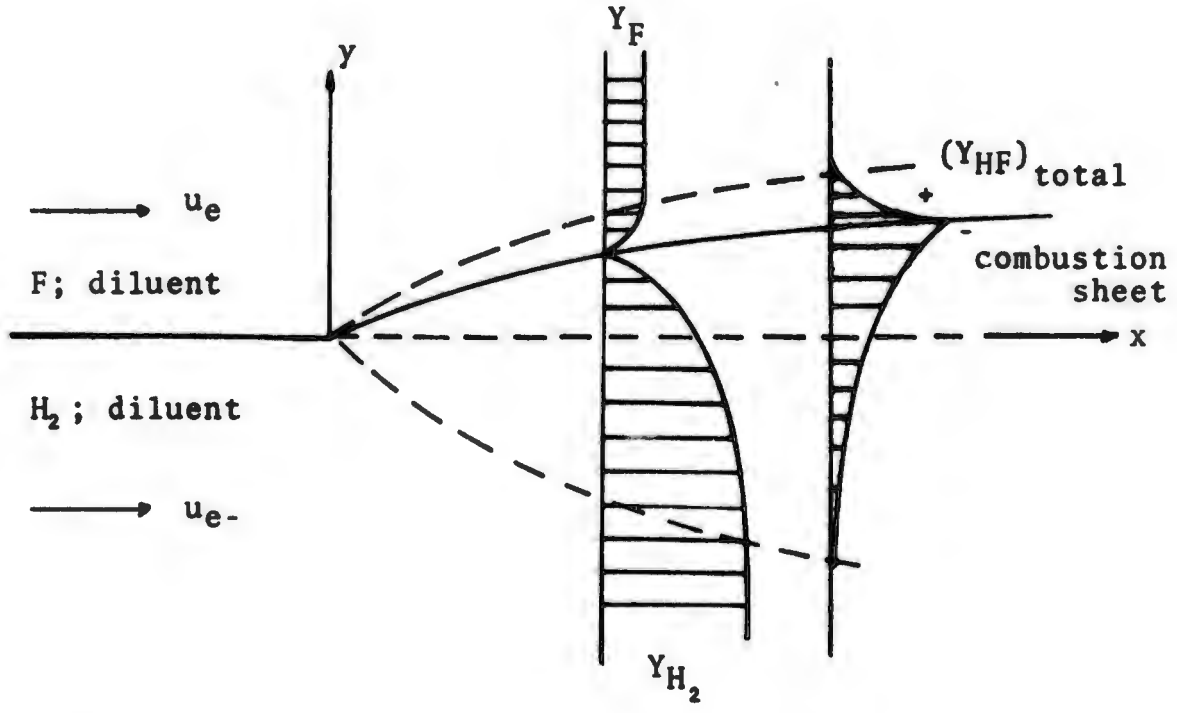

Fig. 1. Semi-Infinite Stream Configuration

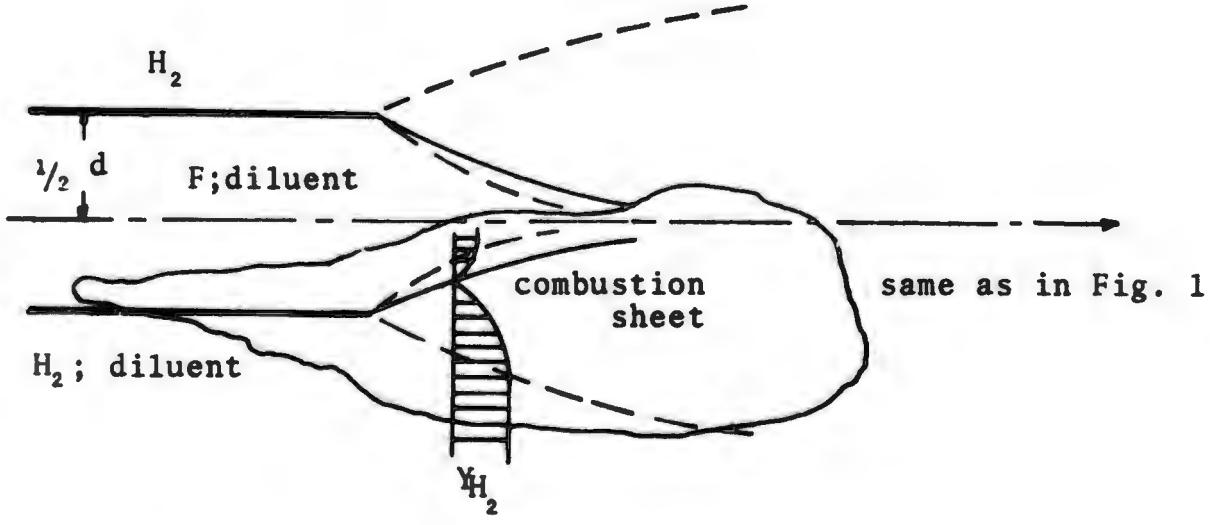

Fig. 2. Nozzle Configuration

APPENDIX A

Influence of Higher Vibrational Levels – Effect of the Hot Reaction $H+F_2 \rightarrow HF+F$

The intent here is to outline the main steps which are required to extend the foregoing theory by including the hot reaction $H+F_2 \rightleftarrows HF+F$. This reaction, unlike the cold reaction $H_2+F \rightleftarrows HF+H$, contributes heavily to the pumping of vibrational levels four through six. The flow configuration is sketched in Fig. A-1 and shows that the upper stream is now the carrier of two oxydizers, namely, F and F_2. The lower stream is assumed to contain the fuels H and H_2.

The mixture is taken to consist of the species HF(0), HF(1),.....HF(6), H_2, F, H, F_2, and diluents D_1 and D_2, numbered respectively from zero to twelve. The chemistry of the system is assumed to be governed by the following reactions:

Reactions		a	b	c °K
0.	$H_2 + F \underset{k_{b,0}}{\overset{k_{f,0}}{\rightleftharpoons}} HF(0) + H$	$0.7 \cdot 10^{13}$	0	860
1.	$H_2 + F \rightarrow HF(1) + H$	$1.4 \cdot 10^{13}$ $(2.57 \cdot 10^{13})$	0	860 (810)
2.	$H_2 + F \rightarrow HF(2) + H$	$7.0 \cdot 10^{13}$ $(9.05 \cdot 10^{13})$	0	860 (810)
3.	$H_2 + F \rightarrow HF(3) + H$	$0.7 \cdot 10^{13}$ $(4.4 \cdot 10^{13})$	0	860 (810)
0'.	$H + F_2 \overset{k'_{f,0}}{\rightarrow} HF(0) + F$	$0.11 \cdot 10^{13}$	0	1200

(A1)

1'.	$H + F_2 \rightarrow HF(1) + F$	$0.25 \cdot 10^{13}$	0	1200
2'.	$H + F_2 \rightarrow HF(2) + F$	$0.35 \cdot 10^{13}$	0	1200
3'.	$H + F_2 \rightarrow HF(3) + F$	$0.36 \cdot 10^{13}$	0	1200
4'.	$H + F_2 \xrightarrow{k'_{f,4}} HF(4) + F$	$1.63 \cdot 10^{13}$	0	1200
5'.	$H + F_2 \rightarrow HF(5) + F$	$3.62 \cdot 10^{13}$	0	1200
6'.	$H + F_2 \rightarrow HF(6) + F$	$4.81 \cdot 10^{13}$	0	1200
1''.	$HF(1) + M \xrightarrow{k''_{f,1}} HF(0) + M$	$0.5 \cdot 10^{8}$	1.3	0
2''.	$HF(2) + M \rightarrow HF(1) + M$	$1.0 \cdot 10^{8}$	1.3	0
3''.	$HF(3) + M \rightarrow HF(2) + M$	$1.5 \cdot 10^{8}$	1.3	0
4''.	$HF(4) + M \rightarrow HF(3) + M$	$2.0 \cdot 10^{8}$	1.3	0
5''.	$HF(5) + M \rightarrow HF(4) + M$	$2.5 \cdot 10^{8}$	1.3	0
6''.	$HF(6) + M \rightarrow HF(5) + M$	$3.0 \cdot 10^{8}$	1.3	0

(A1)

Reactions 0-3 specify the pumping rates generated by the cold reaction which distributes the HF products among levels zero through three.[1] Examination of the hot reaction rate constants shows that over 90 percent of the total production rate is associated with levels four through six. Moreover,

---

[1] Values given in parentheses were those supplied to the author by W. A. Martin of AMICOM. The same statement applies to all other rates in the table.

the values of "a" connected with reactions 0'-3' are almost an order of magnitude smaller than those given by the cold reaction. On this basis, it seems plausible to neglect (ultimately) reactions 0'-3'. Actually, neglecting reactions 0'-3' is dictated more by the resulting mathematical simplifications. Reactions 1''-6'' represent vibration-translation transfers. In accord with the main part of the report, vibration-vibration interactions are not considered.

The system of diffusion equations which parallels (6)-(13) in the text is as follows:

$$\rho u(Y_0)_x + \rho v(Y_0)_y - [\rho D(Y_0)_y]_y = \rho^2 k_{f,0} \frac{Y_{N_2}}{M_{N_2}} \frac{Y_F}{M_F} M_{HF} + \rho^2 k'_{f,0} \frac{Y_H}{M_H} \frac{Y_{F_2}}{M_{F_2}} M_{HF} + \rho^2 k''_{f,1} \frac{Y_1}{M_{HF}} \frac{Y_C}{M_C} M_{HF} - 0 \qquad \text{(A2)}$$

$$\rho u(Y_1)_x + \rho v(Y_1)_y - [\rho D(Y_1)_y]_y = \rho^2 k_{f,1} \frac{Y_{N_2}}{M_{N_2}} \frac{Y_F}{M_F} M_{HF} + \rho^2 k'_{f,1} \frac{Y_H}{M_H} \frac{Y_{F_2}}{M_{F_2}} M_{HF} + \rho^2 k''_{f,2} \frac{Y_2}{M_{HF}} \frac{Y_C}{M_C} M_{HF} - \rho^2 k''_{f,1} \frac{Y_1}{M_{HF}} \frac{Y_C}{M_C} M_{HF} \qquad \text{(A3)}$$

$$\rho u(Y_2)_x + \rho v(Y_2)_y - [\rho D(Y_2)_y]_y = \rho^2 k_{f,2} \frac{Y_{N_2}}{M_{N_2}} \frac{Y_F}{M_F} M_{HF} + \rho^2 k'_{f,2} \frac{Y_H}{M_H} \frac{Y_{F_2}}{M_{F_2}} M_{HF} + \rho^2 k''_{f,3} \frac{Y_3}{M_{HF}} \frac{Y_C}{M_C} M_{HF} - \rho^2 k''_{f,2} \frac{Y_2}{M_{HF}} \frac{Y_C}{M_C} M_{HF} \qquad \text{(A4)}$$

$$\rho u(Y_3)_x + \rho v(Y_3)_y - [\rho D(Y_3)_y]_y = \rho^2 k_{f,3} \frac{Y_{N_2}}{M_{N_2}} \frac{Y_F}{M_F} M_{HF} + \rho^2 k'_{f,3} \frac{Y_H}{M_H} \frac{Y_{F_2}}{M_{F_2}} M_{HF} + \rho^2 k''_{f,4} \frac{Y_4}{M_{HF}} \frac{Y_C}{M_C} M_{HF} - \rho^2 k''_{f,3} \frac{Y_3}{M_{HF}} \frac{Y_C}{M_C} M_{HF} \qquad \text{(A5)}$$

$$\rho u(Y_4)_x + \rho v(Y_4)_y - [\rho D(Y_4)_y]_y = 0 + \rho^2 k'_{f,4} \frac{Y_H}{M_H} \frac{Y_{F_2}}{M_{F_2}} M_{HF} + \rho^2 k''_{f,5} \frac{Y_5}{M_{HF}} \frac{Y_C}{M_C} M_{HF} - \rho^2 k''_{f,4} \frac{Y_4}{M_{HF}} \frac{Y_C}{M_C} M_{HF} \qquad \text{(A6)}$$

$$\rho u(Y_5)_x + \rho v(Y_5)_y - [\rho D(Y_5)_y]_y = 0 + \rho^2 k'_{f,5} \frac{Y_H}{M_H} \frac{Y_{F_2}}{M_{F_2}} M_{HF} + \rho^2 k''_{f,6} \frac{Y_6}{M_{HF}} \frac{Y_C}{M_C} M_{HF} - \rho^2 k''_{f,5} \frac{Y_5}{M_{HF}} \frac{Y_C}{M_C} M_{HF} \qquad \text{(A7)}$$

$$\rho u(Y_6)_x + \rho v(Y_6)_y - [\rho D(Y_6)_y]_y = 0 + \rho^2 k'_{6,6} \frac{Y_H}{m_H} \frac{Y_{F_2}}{m_{F_2}} m_{HF} + \quad 0 - \rho^2 k''_{6,6} \frac{Y_6}{m_{HF}} \frac{Y_6}{m_6} m_{HF} \qquad \text{(A8)}$$

$$\rho u(Y_{H_2})_x + \rho v(Y_{H_2})_y - [\rho D(Y_{H_2})_y]_y = -\rho^2 \sum_{\nu=0}^{3} k_{6,\nu} \frac{Y_{H_2}}{m_{H_2}} \frac{Y_F}{m_F} m_{H_2} \qquad \text{(A9)}$$

$$\rho u(Y_F)_x + \rho v(Y_F)_y - [\rho D(Y_F)_y]_y = -\rho^2 \sum_{\nu=0}^{3} k_{6,\nu} \frac{Y_{H_2}}{m_{H_2}} \frac{Y_F}{m_F} m_F + \rho^2 \sum_{\nu=4}^{6} k'_{6,\nu} \frac{Y_H}{m_H} \frac{Y_{F_2}}{m_{F_2}} m_F \qquad \text{(A10)}$$

$$\rho u(Y_H)_x + \rho v(Y_H)_y - [\rho D(Y_H)_y]_y = \rho^2 \sum_{\nu=0}^{3} k_{6,\nu} \frac{Y_{H_2}}{m_{H_2}} \frac{Y_F}{m_F} m_H - \rho^2 \sum_{\nu=4}^{6} k'_{6,\nu} \frac{Y_H}{m_H} \frac{Y_{F_2}}{m_{F_2}} m_H \qquad \text{(A11)}$$

$$\rho u(Y_{F_2})_x + \rho v(Y_{F_2})_y - [\rho D(Y_{F_2})_y]_y = -\rho^2 \sum_{\nu=4}^{6} k'_{6,\nu} \frac{Y_H}{m_H} \frac{Y_{F_2}}{m_{F_2}} m_{F_2} \qquad \text{(A12)}$$

$$\rho u(Y_{11})_x + \rho v(Y_{11})_y - [\rho D(Y_{11})_y]_y = 0 \qquad \text{(A13)}$$

$$\rho u(Y_{12})_x + \rho v(Y_{12})_y - [\rho D(Y_{12})_y]_y = 0 \qquad \text{(A14)}$$

In (A2)-(A14), the first seven equations govern the kinetics and flow of the active species and the remaining equations describe, respectively, the behavior of H_2, F, H, F_2 and the diluents D_1 and D_2.

Since reactions 0'-3' are now neglected, it is possible to effectively separate the action of the hot reaction from that of the cold reaction. This is reflected in the definitions

$$(Y_{HF,tot})_\ell \equiv \sum_{v=0}^{3} Y_{HF,v} \tag{A15}$$

and

$$(Y_{HF,tot})_h \equiv \sum_{v=4}^{6} Y_{HF,v} \tag{A16}$$

where ℓ denotes "lower" and h denotes "higher." As in the text, let $Y^{\circ}_{HF,v}$ denote the HF mass fractions when collisional deactivation is neglected. Then, summing (A2) through (A5) and (A6) through (A8) yields, in accord with the foregoing definitions,

$$\rho u\left[(Y^{\circ}_{HF,tot})_\ell\right]_x + \rho v\left[(Y^{\circ}_{HF,tot})_\ell\right]_y - \left\{\rho D\left[(Y^{\circ}_{HF,tot})_\ell\right]_y\right\}_y = \rho^2 \sum_{v=0}^{3}{}' k_{\ell,v} \frac{Y_{M_\ell}}{M_{M_\ell}} \frac{Y_F}{M_F} M_{HF} \tag{A17}$$

and

$$\rho u\left[(Y^{\circ}_{HF,tot})_h\right]_x + \rho v\left[(Y^{\circ}_{HF,tot})_h\right]_y - \left\{\rho D\left[(Y^{\circ}_{HF,tot})_h\right]_y\right\}_y = \rho^2 \sum_{v=4}^{6}{}' k_{\ell,v} \frac{Y_H}{M_H} \frac{Y_{F_2}}{M_{F_2}} M_{HF}. \tag{A18}$$

Comparison of equations (A2)-(A8) with the collisional deactivation terms neglected and equations (A17) and (A18) yields

$$(Y^{\circ}_{HF,v})_\ell = f_{v,\ell}\,(Y^{\circ}_{HF,tot})_\ell \qquad v = 0, \ldots 3, \tag{A19}$$

and

$$(Y^{\circ}_{HF,v})_h = f_{v,\ell}\,(Y^{\circ}_{HF,tot})_h \qquad v = 4, \ldots 6, \tag{A20}$$

where

$$f_{v,\ell} \equiv \frac{k_{\ell,v}}{\sum_{v=0}^{v=5} k_{\ell,v}} \tag{A21}$$

and

$$f_{v,h} \equiv \frac{k'_{\ell,v}}{\sum_{v=4}^{6} k'_{\ell,v}} . \tag{A22}$$

The overall distribution factor $f_{v,tot}$ is given by

$$f_{v,tot} = \frac{f_{v,\ell}\,(Y^{\circ}_{HF,tot})_{\ell} + f_{v,h}\,(Y^{\circ}_{HF,tot})_{h}}{Y^{\circ}_{HF,tot}} \tag{A23}$$

where

$$Y^{\circ}_{HF,tot} \equiv (Y^{\circ}_{HF,tot})_{\ell} + (Y^{\circ}_{HF,tot})_{h} . \tag{A24}$$

Clearly, $Y^{\circ}_{HF,tot} = Y_{HF,tot}$ which is to say that collisional deactivation (and radiative interactions) leave the total HF mass fraction unaltered.

The simplest situation involving six vibrational levels is examined, namely the one resulting from combustion of fuels and oxydizers in a single flame sheet, Fig. A-1. In this case, most of the results given in the text carry over intact. The few changes and generalizations that are required are summarized in the next few paragraphs.

The system of equations (44)-(51) remains unchanged, provided it is understood that: (48) stands for two equations —one for $(Y^{\circ}_{HF,tot})_{\ell}$ and the other for $(Y^{\circ}_{HF,tot})_{h}$ — and an equation of the form (46) governing the behavior of F_2 is added. The same is true of the zero order solutions (55)-(61) so long as it is understood that: to (58),which formally

stands for $(Y^{\circ}_{HF,tot})_1$, two otherwise identical solutions for $(Y^{\circ}_{HF,tot})_h$ are added, a solution for Y_{F_2} formally identical to (56) is added, (57a) is deleted and the normalizing factor in (57b) is taken to be Y_{H_e-}. An additional stoichiometric flux requirement paralleling (62) is necessary, namely:

$$-\frac{1}{m_H} Y_H' \Big|_- = \frac{1}{m_{F_2}} Y_{F_2}' \Big|_+ . \tag{A25}$$

This statement yields a second condition on f_*' paralleling (67). The two expressions must be equal and therefore

$$\frac{m_{H_2} Y_{F,e} \Lambda + m_F Y_{H_2,e^-}}{Y_{H_2,e} m_F + Y_{F,e} m_{H_2}} = \frac{m_H Y_{F_2,e} \Lambda + m_{F_2} Y_{H,e^-}}{Y_{H,e} m_{F_2} + Y_{F_2,e} m_H} \tag{A26}$$

must hold. This means that not all four ambient mass fractions appearing in (A26) can be prescribed arbitrarily. For example, if no diluents are present, then any three can be specified and the fourth is set by (A26) together with

$$Y_{F_2,e} + Y_{F,e} = 1 , \quad Y_{H_2,e} + Y_{H,e} = 1 . \tag{A27}$$

This is a peculiarity of the single flame front combustion model involving two reactions. The current model also differs from the one described in the text in that condition (63) is abandoned for both the hot and cold reactions. Now, in the text, (63) implied equality of mole fractions of the reaction products and the interface mass balance (73) was satisfied identically. Herein, the overall interface mass flux balance

$$-Y_{H_2}' \Big|_- - Y_H' \Big|_- + Y_{F_2}' \Big|_+ + Y_F' \Big|_+ = -(Y_{HF,tot}')_2 \Big|_+ + (Y_{HF,tot}')_2 \Big|_- - (Y_{HF,tot}')_1 \Big|_+ + (Y_{HF,tot}')_1 \Big|_- \tag{A28}$$

together with

$$(Y^{\bullet}_{HF,tot})_{l,s} + (Y^{o}_{HF,tot})_{k,s} = (Y^{o}_{HF,tot})_{s} = (Y_{HF,tot})_{s} \qquad (A29)$$

is taken to determine compatible interface mass fraction of $Y_{HF,tot}$. (For the sake of simplicity, the influence of the diluents is again disregarded.) The reason is that the current model cannot distinguish as to what goes on in the combustion sheet itself with regard to F generated by the hot reaction and consumed by the cold reaction and H generated by the cold reaction and consumed by the hot reaction. Otherwise, the zero order solutions represent the same type of a limiting situation described in 2.1 of the text. Of course, the flame sheet flow field is now set by the magnitudes of seven $\zeta_{p,v}$'s and six ζ_{cd}'s of the kind given in (37) and (38).

The foregoing development clearly indicates that the perturbation scheme developed in Section 2.4 of the text may be carried over to the current system with obvious and minor modifications. The same is true of most of the material in Section (2.5). For example, the general form representing the six diffusion equations which govern the distribution of the active species with radiation included is

$$(Y_{HF,v})_{\eta\eta} + Sc f(Y_{HF,v})_{\eta} + Sc\frac{2x}{u_e}\rho k_{f,v}\frac{Y_{H_2}}{M_{H_2}}\frac{Y_F}{M_F}M_{HF} + Sc\frac{2x}{u_e}\rho k'_{f,v}\frac{Y_H}{M_H}\frac{Y_{F_2}}{M_{F_2}}M_{HF} + Sc\frac{2x}{u_e}\rho k''_{f,v+1}\frac{Y_{HF,v+1}}{M_{HF}}\frac{Y_c}{M_c}M_{HF}$$

$$- Sc\frac{2x}{u_e}\rho k''_{f,v}\frac{Y_{HF,v}}{M_{HF}}\frac{Y_c}{M_c}M_{HF} + Sc\frac{2x}{u_e}u_{v;v,v+1}\frac{\Theta_R}{T}B_{v,v+1}(2j_{v+1}+3)e^{-(j_{v+1}+1)(j_{v+1}+2)\frac{\Theta_R}{T}}\left(Y_{HF,v+1}e^{\frac{2\Theta_R}{T}(j_{v+1}+1)} - Y_{HF,v}\right) \qquad (A30)$$

$$+ Sc\frac{2x}{u_e}u_{v;v-1,v}\frac{\Theta_R}{T}B_{v-1,v}(2j_v+3)e^{-(j_v+1)(j_v+2)\frac{\Theta_R}{T}}\left(Y_{HF,v}e^{\frac{2\Theta_R}{T}(j_v+1)} - Y_{HF,v-1}\right) = 2Sc\,s\left[f_q(Y_{HF,v})_s - f_s(Y_{HF,v})_q\right]$$

where $v = 0,\ldots 6$ and where it is understood that $Y_{HF,v+1}$ and $k''_{f,v+1}$ are identically zero for $v = 6$. For the flame sheet model, the right-hand side of (A30) is zero. Moreover, in the limiting case of a saturated medium (see Section 2.5 of the text), the active species satisfy the relationship

$$(Y_{HF,v})_{sat}\, e^{2(i_v+1)\frac{\Theta_R}{T}} = (Y_{HF,v-1})_{sat}. \qquad \text{(A31)}$$

Equation (A31) is based upon the rotational equilibrium assumption. In this equation, the temperature may be approximately taken to be that given by the zero order solutions. Power output may then be estimated as noted in the text.

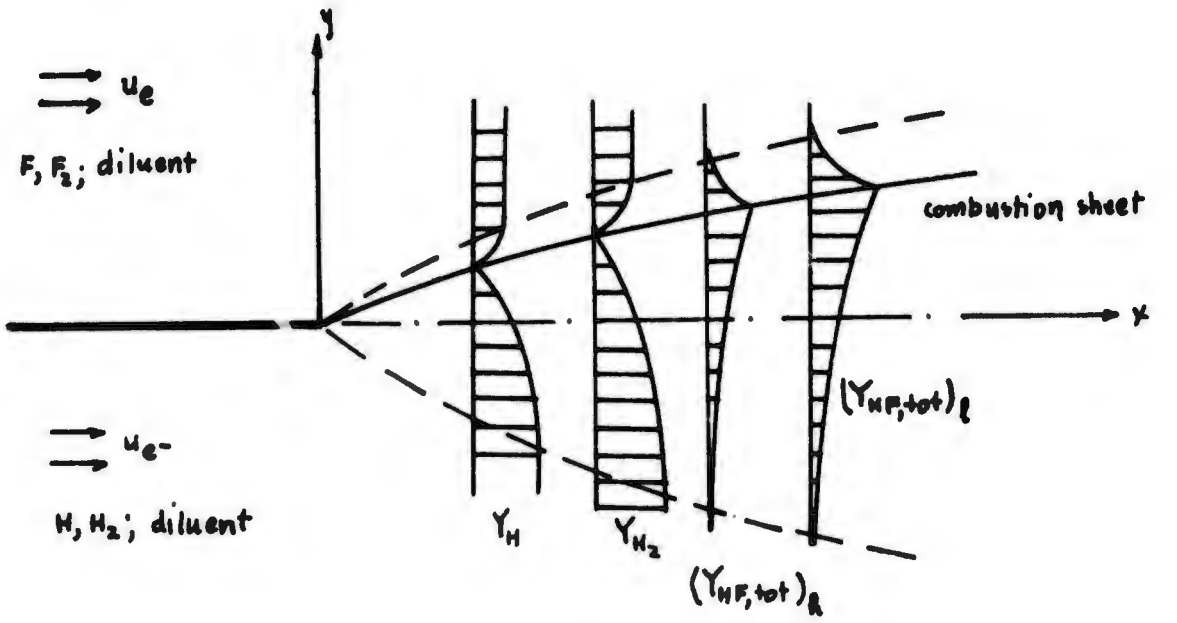

Fig. A-1. Semi-Infinite Stream Configuration

NOMENCLATURE

A_{ul}	-	Einstein coefficient for spontaneous emission
a	-	constant related to reaction rates, Eq.1
B_{lu}	-	Einstein coefficient for absorption ($cm^3/erg\ sec^2$)
B_{ul}	-	Einstein coefficient for stimulated emission
B_{ref}	-	reference value for the Einstein coefficients
b_D	-	Doppler halfwidth of a line, Eq.59
c	-	constant related to reaction rates, speed of light
D	-	effective diffusion coefficient for the multicomponent mixture
f	-	dimensionless stream function of the Blasius type
h	-	Planck's constant
j_v	-	rotational quantum number of the upper level of the transition $v,j_v \rightarrow v-1,j_v+1$
j	-	rotational quantum number
$k_{f,i}$	-	forward rate of the i^{th} reaction, Eq.1
l_v^+, l_v^-	-	fractions of populations of the vibrational levels associated with the j^{th} rotational levels
M_i	-	molecular weight of the i^{th} specie
m	-	mass of the HF molecule, Eq. 65

Preceding page blank

N_A - Avogadro's number

N - total number of species

n - number of molecules per unit volume

p - - pressure

$\langle R_L \rangle$ - line radiancy

Sc - Schmidt number

T - temperature

u - x-component of flow velocity

u_ν - spectral energy density

$u_{\nu,v,v-1}$ - u_ν value for the transition v→v-1

v - y-component of flow velocity; vibrational level v

$\dot{w}_i$ - net mass rate of production of species i per unit volume

x - streamwise distance

Y^i or Y_i - mass fraction of the i^{th} specie

$\bar{Y}^i$ or $\bar{Y}_i$ - normalized mass fraction

Greek Symbols

$\hat{\alpha}_v$ - integrated gain coefficient for the transition v→v-1

β_v - $B_{v-1,v}/B_{ref}$

ζ - symbol for several Damkohler numbers

$\zeta_{p,i}$ - pumping Damkohler number based on the diffusion equation for the i^{th} specie

$\zeta_{cd,i}$ - collisional deactivation Damkohler number based on the diffusion equation for the i^{th} specie

$\zeta_{r,i}$ - radiative Damkohler number

$\eta, \bar{\eta}$ - boundary layer similarity variables

Θ, Θ_R - $T/T_{ref} \equiv T/T_*^\circ$; characteristic rotational temperature

λ_v - distribution function for the intensity among the active lines.

ρ - density of the mixture (gm/cm^3)

τ - one of several characteristic times

Subscripts

c - denotes a collision partner in a V-T transfer or the associated mass fraction Y_c

cd - denotes collisional deactivation

e - denotes edge of mixing layer on the fluorine side

e- - denotes edge of mixing layer on the hydrogen side

i - refers to species

j - rotational level

p - refers to chemical pumping

r - refers to radiation

tot - denotes "total" - total mass fraction of HF

u - upper level

ul - upper level to lower level

v	-	vibrational level v
*	-	refers to flame sheet

Superscripts

i	-	denotes i^{th} specie, Section 2.2
o or (o)	-	refers to zero order solutions
',,"	-	refers to conditions after lasing, Section 2.3; also a symbol for $\frac{d}{d\eta}$

Numbering of species: from 0-8, respectively, HF(0), HF(1), HF(2), HF(3), H_2, F, H, D_1 (diluent in F-stream), D_2 (diluent in H_1-stream)

END